Emerging advances and current applications of nanoMOF-based membranes for water treatment

M.S. Attia, A.O. Youssef, Mona Abou-Omar, Ekram Mohamed, Rabah Boukherroub, Afrasyab Khan, Tariq Altalhi, Mohammed Amin

Chemosphere xxx (xxxx) 133369

Contents lists available at ScienceDirect

Chemosphere

journal homepage: www.elsevier.com/locate/chemosphere

Emerging advances and current applications of nanoMOF-based membranes for water treatment

M.S. Attia [a, **], A.O. Youssef [a], Mona N. Abou-Omar [b], Ekram H. Mohamed [c], Rabah Boukherroub [d], Afrasyab Khan [e], Tariq Altalhi [f], Mohammed A. Amin [f, *]

[a] Chemistry Department, Faculty of Science, Ain Shams University, Cairo, 11566, Egypt
[b] Department of Chemistry, Faculty of Women for Arts, Science and Education, Ain Shams University, Cairo, Egypt
[c] Pharmaceutical Analytical, Chemistry Department, Faculty of Pharmacy, The British University in Egypt, 11837, El Sherouk City, Cairo, Egypt
[d] Univ. Lille, CNRS, Centrale Lille, Univ. Polytechnique Hauts-de-France, UMR 8520, IEMN, F-59000, Lille, France
[e] Institute of Engineering and Technology, Department of Hydraulics and Hydraulic and Pneumatic Systems, South Ural State University, Lenin Prospect 76, Chelyabinsk, 454080, Russian Federation
[f] Department of Chemistry, College of Science, Taif University, P.O. Box 11099, Taif, 21944, Saudi Arabia

ARTICLE INFO

Handling Editor: Chang-Ping Yu

Keywords:
NanoMOF
NanoMOF-based membrane
Water treatment
Nano-scale MOF
Composite membrane

ABSTRACT

Metal-organic frameworks (MOFs) are significantly tunable materials that can be exploited in a wide range of applications. In recent years, a large number of studies have been focused on synthesizing nano-scale MOFs (nanoMOFs), thus taking advantage of these unique materials in various applications, especially those that are only possible at nano-scale. One of the technologies where nanoMOF materials occupy a central role is the membrane technology as one of the most efficient separation techniques. Therefore, numerous reports can be found on the enhancement of the physiochemical properties of polymeric membranes by using nanoMOFs, leading to remarkably improved performance. One of the most considerable applications of these nanoMOF-based membranes is in water treatment systems, because freshwater scarcity is now an undeniable crisis facing humanity. In this in-depth review, the most prominent synthesis and post-synthesis methods for the fabrication of nanoMOFs are initially discussed. Afterwards, different nanoMOF-based composite membranes such as thin-film nanocomposites (TFN) and mixed-matrix membranes (MMM) and their various fabrication methods are reviewed and compared. Then, the impacts of using MOFs-based membranes for water purification through growing metal-organic frameworks crystals on the support materials and utilization of metal-organic frameworks as fillers in mixed matrix membrane (MMM) are highlighted. Finally, a summary of pros and cons of using nanoMOFs in membrane technology for water treatment purposes and clear future prospects and research potentials are presented.

1. Introduction

Nanotechnology has been a huge step toward achieving results that seemed inaccessible earlier. More specifically, synthetic nanomaterials that are highly adjustable exhibiting outstanding properties can have widespread applications in different scientific fields (Gajanan and Tijare,2018; Ghasemzadeh et al., 2014; Kahn et al., 2017) Using these kinds of materials, engineering at the nano-scale can be possible and desired results can be achieved. Ever since the advent of this technology, various synthetic methods were developed for the fabrication of a wide range of nanomaterials with different properties that can be utilized for specific applications. It is really difficult to name all the possible applications of nanomaterials, but as the most prominent fields, biomedical imaging (Han et al., 2019; Nune et al.,2009) separation technologies (e.g. membrane and adsorption processes) (liu et al.,2019; Palit, 2016), analytical and environmental applications (Fraceto et al., 2018; Xie et al.,2012), medical applications (e.g. drug delivery) (Fazal-ur-Rehman, 2018, Saeedi et al., 2019), chemical sensors (Bhushan et al., 2007; Talebian et al., 2020), metallurgy (Ross et al., 2016; Tang et al., 2019), and electronic (Hester et al., 2015; Lee et al., 2019) can be mentioned.

Metal-organic frameworks (MOFs), also known as porous coordination polymers (PCP), are one of the most prominent and emerging mod-

* Corresponding author.
** Corresponding author.
E-mail addresses: mohd_mostafa@sci.asu.edu.eg (M.S. Attia), mohamed@tu.edu.sa (M.A. Amin).

https://doi.org/10.1016/j.chemosphere.2021.133369
Received 4 July 2021; Received in revised form 28 November 2021; Accepted 17 December 2021
0045-6535/

ular nanomaterials. These materials are composed of inorganic clusters linked by organic ligands. By choosing appropriate inorganic and organic components in the synthesis step, MOF nanoparticles with desired chemical functionality and crystalline structure can be produced (Kitagawa, 2014). Overall, due to their unique properties such as well-defined 3D structure, permanent porosity with completely adjustable pores, and diverse chemical functionalities, MOFs have gained extensive attention and numerous computational and experimental studies have been reported so far (Cai et al., 2020). Applications of MOFs in membranes (Lin et al., 2018; Kadhom and Deng, 2018), gas storage and separation (Liu et al., 2019a, Li et al., 2014), drug delivery (Cai et al., 2019a; Zhuang et al., 2014), chemical sensing (Stassen et al., 2017; Yi et al., 2016), and catalysis (Chen et al., 2018; Gascon et al., 2014) are the major examples to be mentioned. According to the literature, there is a meaningful relationship between the structure and functionality of MOFs (Wang et al.,2018a,b.c). Therefore, various synthetic and post-synthetic methods should be examined ~~in the way of~~ achieving the desired properties. In contrast to the conventional organic and inorganic nanomaterials, the major mechanisms that affect the structure-function relationship of MOFs are not completely discovered and more research is needed. Properties such as permanent porosity, uniform pore size, well-defined surface chemistry, controllable crystalline structure, cellular uptake, and catalytic activity have prominent influence on the application of these materials (Stylianou et al.,2011, Zhang et al.,2020).

As mentioned earlier, membrane technology is one of the most prominent areas that has been broadly taking advantage from MOF nanomaterials to enhance the process efficiency. Membranes, especially the polymeric ones, due to their relatively low cost, high separation efficiency, suitability for a broad-spectrum of applications, flexibility, adjustability, etc. are always of great importance when it comes to the separation technology (Warsinger et al.,2018; Zahid et al., 2018). Generally, MOF-based membranes can be produced in two forms: freestanding MOF membranes based on a template and composite polymeric membranes consisting of MOFs-doped polymer (Qiu et al., 2014). The free-standing MOF membranes are mainly used for gas separation and provide excellent separation performance (Ismail et al., 2015; Peng et al.,2017). Unfortunately, these membranes exhibit high fragility and low permeability, which can limit their applications (Liu et al., 2017). On the other hand, the composite membranes containing MOFs are a group of membranes composed of a polymeric matrix containing MOFs dispersed in it or a MOF coating based on a thin film (Liu et al., 2017a). Due to the compatibility between polymeric chains and MOFs, a good dispersion and stable membrane can be achieved. Among these kinds of membranes, nanoMOF-based membranes due to their standard thickness (≤100 nm), uniform dispersion of MOFs and consequently better stability and simultaneously high selectivity and permeability, have shown outstanding results (Li et al., 2020a). Although the appearance and further development of MOF membranes were only regarded to gaseous systems, recent years witnessed development of MOF-based membranes for liquid systems (Jun et al., 2020). Water as the most vital liquid on this planet, which is also scarce in vast areas, is always one of the most important species to be separated from different contaminants. Based on these useful summary facts, evaluating the capability of MOF membranes for water treatment can be a major field of study in membrane and more generally in separation technology. Studying the various aspects of utilizing membrane technology in water and wastewater treatments has been an important research field in both water and separation technologies (Quist-Jensen et al., 2015). Owing to the nature, physical and chemical properties of water molecules, it is possible to use a semi-permeable network called membrane in order to separate water from various unwanted dissolved species. A membrane with high selectivity, especially in case that the product is expected to be an ultra-pure water, is an essential demand. Because of their uniform and tunable pores, nanoMOF composite membranes can have huge potentials to be used for this purpose to maintain both selectivity and permeability at an acceptable level (Akbari and Peyravi,2020). However, the final performance of the membranes critically depends on the structural characteristics and water-stability of the MOF nanoparticles, which can be controlled through different synthetic and post-synthetic techniques (Wang et al., 2018a,b). Up to now, various nanoMOFs were used as the pore formers and fillers in polymeric composite membranes and their applications in various membrane-based separation systems were comprehensively evaluated (Gu et al., 2019a; Kumar et al.,2018). Even in some special cases, the membrane properties and performance were enhanced by taking advantage of the inherent defects of MOF nanoparticles such as low water-stability of some MOFs, which is so innovative (Yao et al., 2021; Arjmandi et al.,2020a; Lee et al., 2015; Stock et al., 2011).

This review article is aimed to overview the advantages, disadvantages, special applications, and future perspectives of nanoMOF-based membranes in water treatment. After a comprehensive discussion on the basics of MOFs and membranes individually, including fabrication, modification, and evaluation methods, all the most reliable and recent reports on using nanoMOF-based membranes for water treatment will be presented, discussed, and classified in details. The major goal of this study is to comprehensively elaborate on the pros and cons of these kinds of membranes and give some helpful orientations for future research in this field.

2. Synthesis and functionalization of nanoMOFs

2.1. Synthesis of nanoMOFs

Although the syntheses of nanoMOFs have been widely reported in the literature (Deng et al,2021), the lack of a clear general strategy for the synthesis of uniform MOF nanoparticles has remained a serious challenge (60). The kinetic trapping of MOF nanocrystals of particular sizes depends on the competition between four chemical equilibria (Scheme 1): (1) linker deprotonation; (2) modulator (Mod) deprotonation; (3) linker complexation, and (4) termination. Equilibria with fast forward-direction rates and low reversibility dictate whether MOF particles steadily grow toward bulk phases or arrest quickly to form small nanocrystals. MOF linkers must deprotonate (eqn (1)) before forming metal-linker bonds. Modulators are usually acids, and so must also be deprotonated (eqn (2)). Complexation between metal ions and linkers facilitates particle growth (eqn (3)).

Reports suggest that early in MOF growth, large collections of molecular complexes and oligomers develop in solution before coalescing into MOF particles (Lim et al.,2015). Subsequent MOF growth is then dominated by the diffusion of oligomer clusters or solvated reactant molecules. During the termination step (eqn (4)), linker and modulator ligands compete for metal ion coordination sites (Haque and S. H. Jhung, 2011). According to the kinetic model in (Marshall et al.,2019), this process continues until the local concentration of ligands far exceeds the metal ions, thereby arresting particle growth. In addition to these four chemical processes, the assembly of cluster nodes and solvent decomposition have also been invoked to discuss nano-MOF nucleation and growth (Surbl´e et al.,2006), but we focus on the most general processes that dominate particle trapping. Critical analysis of nano-

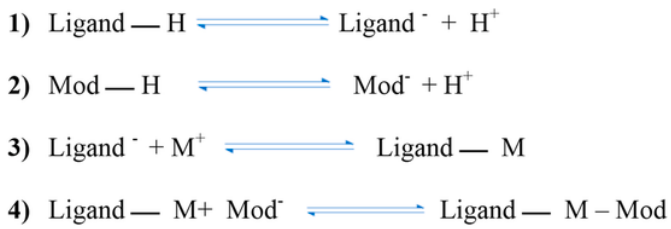

Scheme 1. Key chemical equilibria controlling nano-MOF growth and termination.

MOF sizes and synthetic conditions reveals the existence of key parameters that may be programmed to deplete local concentrations of metal ions and generate small particle sizes: modulator identity and concentration, equivalents of linker or modulator, and metal–ligand bond strengths.

Modulators. Modulators are typically monotopic carboxylic acids and occasionally Brønsted bases added for the synthesis of nano-MOFs. The intended purpose of modulators varies, but it is believed that their function is to influence nano-MOF sizes by affecting linker deprotonation and arresting particle growth (Diring et al.,2010). Modulators also act to prevent particle aggregation. Although modulators produce size trends that appear complex and contradictory, their role can be rationalized in terms of the four equilibria outlined above. When strong Brønsted bases are used as modulators, their primary role is to facilitate ligand deprotonation (eqn (1)) and enhance metal-linker complexation (eqn (3)) relative to metal-ion diffusion, thereby depleting local metal ion concentration and forming small MOF nanocrystals. For example, nanocrystals of MFU-4 ($Zn_5Cl_4(BBTA)_3$) decrease in size in presence of lutidine or KOH (Ettlinger et al., 2018). Similarly, when nanocrystals of NU1000 ($Zr6(m3\text{-}OH)_8(OH)_8(TBAPy)_2$) are prepared with the addition of 4-biphenyl-carboxylic acid, particle sizes decrease further if NaOH is added to the precursor linker solution (Webber et al., 2017). Nanocrystals of MOF-5 and IR-MOF-3 ($Zn_4O(TPDC)_3$) require triethylamine (TEA), which become more uniform with initial addition of cetyltrimethylammonium bromide (CTAB) (Maet al., 2011). Similarly, addition of *n*-butylamine decreases nanocrystal size of ZIF-71 ($Zn(Hdcim)_2$) (Haque and S. H. Jhung, 2011). Interestingly, nanoparticles of MIL-101(Cr) ($Cr_3(H_2O)_2O((C_6H_3)\text{-}(CO_2)_3)_2$) are synthesized without any modulator by simply decreasing the amount of HF, which is used as a mineralizing agent in the traditional bulk synthesis (Thi et al., 2018; Yang et al.,2019; Zhang et al., 2018a). Addition of a strong base to the reaction mixture, however, results in smaller particle size (Zhang et al., 2018b). When carboxylic acids serve as modulators, their presence can increase or decrease nano-MOF size, depending on whether they impede linker deprotonation (eqn (1)) or act as surface capping ligands (eqn (4)). By interfering with deprotonation, they slow down metal-linker complexation (eqn (3)) relative to metal-ion diffusion, resulting in large nano-MOF sizes. On the other hand, they can terminate particle growth by acting as surface capping ligands and produce small sizes. Operating under high concentrations of reagents necessitates the addition of a modulator; otherwise, rapid metal-ion diffusion, due to short effective pathlengths, outcompetes growth termination (eqn (4)). Indeed, most nanoscale MOF syntheses rely on dilute conditions. For example, synthesis of MIL-101-Cr involving high concentrations (0.2 M H_2BDC) generates small particle sizes only upon addition of small quantities of benzoic acid (Fig. 1), (Yang et al.,2019a).

The more acidic benzoic acid has a greater effect than acetic acid on decreasing particle size at such high reactant concentrations, suggesting that under these reaction conditions, interfering with metal–ligand complexation is critical to kinetically trapping small MIL-101-Cr nanocrystals. Phase purity must be considered when choosing modulator equivalents and reaction concentrations. For example, while addition of a few equivalents of either acetic or benzoic acid in the synthesis of MIL-101 at high concentrations results in pure phase MIL-101 nanocrystals, greater equivalents induce the formation of mixed-phase products (Zhang et al., 2018a), because MIL-101 and MIL-88B occupy the same reaction space, with both arising from Fe^{3+} or Cr^{3+} and trimesic acid (Thi et al., 2018b). Therefore, at a benzoic acid: linker ratio of 10: 1, only MIL-88B microcrystals form (Yang et al.,2019a). Concentration plays an important role in controlling nanocrystal phase purity as well. For example, MIL-101-Cr and MIL-88B-Fe nano-crystals were obtained with similar equivalents of acetic acid, but the synthesis of MIL-88B-Fe was an order of magnitude more diluted (Fig. 1). Such phase transformations with variable modulator equivalents indicate the importance of nonclassical growth mechanisms (Seoane et al., 2015).

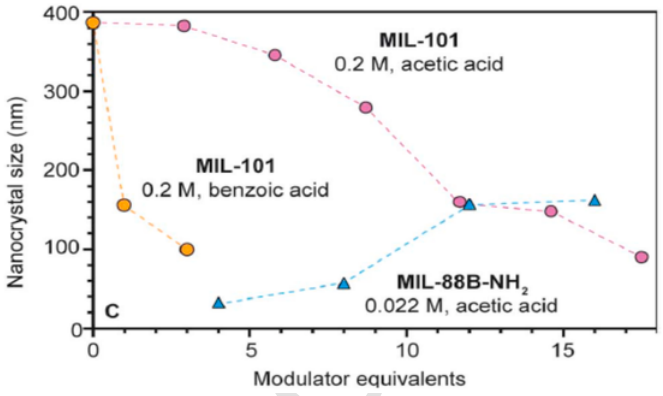

Fig. 1. Nanoscale MOF size depend on the equivalents and pKa values of added modulator reagents: MIL-101-Cr nanocrystal size decreases with increased modulator equivalents, while MIL-88B-NH2-Fe exhibits the opposite trend. Interestingly, MIL-88B microcrystals are formed as an impurity at and above 5 benzoic acid equivalents (orange). Sizes were determined with SEM (orange and pink) and TEM (blue) (Zhang et al., 2018a).

Similar phenomena have been observed for the phase spaces involving MIL-100-Al ($Al_3(H_2O)_2O(BTC)_2$)/MIL-96-Al ($Al_{12}O\text{-}(OH)_{16}(H_2O)_5(BTC)_6$, MIL-110-Al ($Al_8(OH)_{12}(\text{-}OH)_3(H_2O)_3(BTC)_3$) and NU-901 ($Zr_6(m3\text{-}OH)_8(OH)_8(TBAPy)_2$)/NU-1000 (M´arquez et al.,2012; Seoane et al., 2015; Webber et al., 2017).

Linker equivalents. Excess linker equivalents shifts equilibria toward enhanced metal–ligand complexation (eqn (3)), thereby depleting local metal ion concentrations (64) and arresting particle growth without added modulator (eqn (4)). In other words, excess linkers serves as surface-capping ligands. The excess linker method was first reported in 2009 for ZIF-8 and has since been used ~~in~~ further ~~ZIF~~ 8 and ZIF-71 nanocrystal syntheses (Cravillon et al.,2009;, Haque and S. H. Jhung, 2011; Marshall et al.,2019). Nano-MOF particle sizes can be further reduced by adding Brønsted bases to enhance linker deprotonation (eqn (1)) (Cravillon et al.,2009). Irreversible ligand deprotonation may lead, however, to unchecked particle growth through rapid metal–ligand complexation, unless counterbalanced by excess surface capping ligands, illustrating the intricate kinetic balance of the four key underlying processes outlined in eqn (1)–(4). Although several chemical parameters may contribute to decreased nano-MOF sizes, the impact of certain factors may dominate over others. For example, excess of linker was discovered to be the single strongest size determinant of ZIF-8 nano crystals through systematic investigations of the role of Brønsted base, linker excess, and reactant concentrations (Cravillon et al.,2009). Nanocrystals of ZIF-8 can be synthesized using an excess of the 1-methylimidazolium (Hmim) linker (Cravillon et al.,2009), whereas typical bulk syntheses of ZIF-8 combine the zinc salt and imidazole linker in a 1:1 ratio (Cravillon et al.,2009). Simply increasing the metal-to-linker ratio to 1:5 results in nanocrystals sizes of 40 nm (Cravillon et al., 2009). In terms of the kinetic model reported in ref. (Haque and S. H. Jhung, 2011), the role of dilution is to increase metal-ion diffusion pathlengths, allowing particles to be terminated ~~iso~~ ated from additional metal ions. The impact of added base was also assessed, but only the basic modulator *n*-butylamine resulted in reduced nanocrystal sizes, whereas less basic 1-methylimidazole and sodium formate produced micrometer sized crystals (Haque and S. H. Jhung, 2011).

Metal–ligand bond strengths. Strong metal–ligand interactions favor small particle size because they enhance rates of both complexation (eqn (3)) and termination (eqn (4)) during nano-MOF growth, thereby depleting the local concentrations of metal ions relative to linkers or modulators. Systematic studies varying the metal identities of heterobimetallic materials illustrate the influence of metal–ligand interactions on nanocrystal size. For instance, weaker bonds might slow particle growth, allowing diffusing linkers trap the metal variants at smaller

sizes. To date, there have been a few studies regarding the effect of mixed metals on MOF nano crystal size and this area warrants further exploration.

2.1.1. Solvothermal method

The solvothermal synthetic procedure is broadly used for the production of different materials. This method is almost the same as the hydrothermal method except that in this technique a non-aqueous precursor solution is usually used (Lai et al.,2015). Using this approach, almost all the advantages of the sol-gel and hydrothermal methods can be included, thus the size and shape distribution and also the crystallinity of the nano-structured products can be precisely controlled. There are some important empirical variables for controlling the product characteristics using this method including reaction temperature, reaction time, type of solvent, type of surfactant, type of precursor, pH, and stochiometric ratio (Lim et al.,2015). There are some reports on directly synthesizing nanoMOFs such as Fe-MIL-88A (Chalatiet al.,2011) (MIL = Materials of "Institut" Lavoisier), MOF-5 (Hermes et al., 2007), and ZIF-8 (79) (ZIF = Zeolitic Imidazolate Framework) by precisely regulating these variables. However, having a total control on these parameters during the synthesis is not usually possible. This lack of control can result in the agglomeration of nanoMOFs due to their higher surface energy.

To overcome this challenge, using chemical modulators can be a helping hand to achieve more control on the formation process (1). To gain more understanding of the effect of coordination modulators, this is all about competing over the unoccupied coordination sites between the coordination modulators as nonbridging ligands and the bridging linkers, all occurring in the reaction mixture (Cravillon et al.,2009). As a result, chemical modulators can actively affect the size, shape, and uniformity of the nanocrystals through controlling the nucleation sites formed and preferential binding with the specific facets of the crystal (Fig. 2). Kitagawa and co-workers were one of the pioneer groups that used this strategy to optimize the morphology and size of the porous coordination polymer (PCP) nanorods *via* coordination modulation (Tsuruoka et al., 2009). In this study, they used acetic acid as the chemical modulator to directly affect the coordination equilibria and consequently control the growth of $\{Cu_2(ndc)_2(dabco)_n$ PCP nanocrystals. It was demonstrated that the competitive interaction between the coordination mode, used for the framework construction and the acetate-copper, is the dominant factor that controls the reaction rate and the morphology of nanocrystals (Gao et al., 2020). By increasing the concentration of acetic acid, the reaction rate was decreased and the formation of nanorods with high aspect ratios was facilitated. As the summary of the reaction evolution, nanoparticles with an average diameter of about 5 nm, nano cubes with the size of about 80 nm, and nanorods with high aspect ratios were observed after 15, 20, and 30 min, respectively.

Recently, Wang et al. reported a novel synthetic method for the fast and scalable synthesis of nanosized Zirconium (Zn)-, and Hafnium (Hf)-based MOFs (He et al., 2017). In this method, a new strategy was developed through controlling the hydrolysis and nucleation of metal salts in the presence of water and also acetic acid as the coordination modulator regulating the coordinated environment. Synthesis of UiO-66-NH_2 (UiO = Universitetet i Oslo) in this study was considered as an example, in which the precipitation products appeared after just 15 min, which is super-fast compared with the reported conventional method without the presence of water, in which the products started to precipitate after 2 h. Moreover, this fast reaction did not negatively affect the nanoMOF characteristics such as porosity, and chemical and thermal stability. Based on the obtained results, the concentrations of water and acetic acid were the dominant factors affecting the final characteristics. As mentioned, acetic acid acts as the coordination modulator to regulate the coordinated environment between metal ions and ligands. On the other hand, the presence of water was at the origin of the high yield (about 91% based on Zr^{4+}) and fast reaction through the accelerated hydrolysis during the synthetic process, as proved by mass spectrometry (ESI-MS) measurements; in addition, by increasing the concentration of water, the crystallinity of the final products was improved. Accordingly, having water molecules and acetic acid during the synthetic process synergistically induced the formation of octahedral uniform MOF nanoparticles with an average diameter of 200 nm, identical with the conventional method. Importantly, it was proved that this method can be used for synthesizing other types of Zr-MOFs, including BUT-12, PCN-222-Co, UiO-66-$(OH)_2$, UiO-67, UiO-66-2,6-NDC, and UiO-66. More importantly, from the commercial point of view, this synthetic strategy is effective to prepare Zr- and Hf-based nanoMOFs at the gram-scale, which is a remarkable step forward for the production of nanoMOFs for industrial applications.

Another strategy for controlling the particle growth is using surfactants and polymers, which make them part of the nanoMOFs' structure. For instance, polymers such as polyvinylpyrrolidone (PVP) and polyethylene glycol (PEG) can regulate the monodispersity, uniformity, and size of the nanoMOFs (Fig. 3a) (Ayala et al., 2019; Cai et al.,2016; Mejia-Ariza et al.,2016; Uemura et al.,2006, 2003). Synthesis of nanoscale polymer-MOFs by taking advantage from this strategy was reported by Johnson et al. (Fig. 3b-e) (Gu et al.,2019). In this study, contrary to the aforementioned methods, organic linker was first coupled with the PEG methyl ether azide polymer before adding coordination modulators. Generally, it was found that the polymer chain can directly affect the product size and this was reduced by increasing the molecular weight. Considering the synthesis of poly-MOF-5 in this study as an ex-

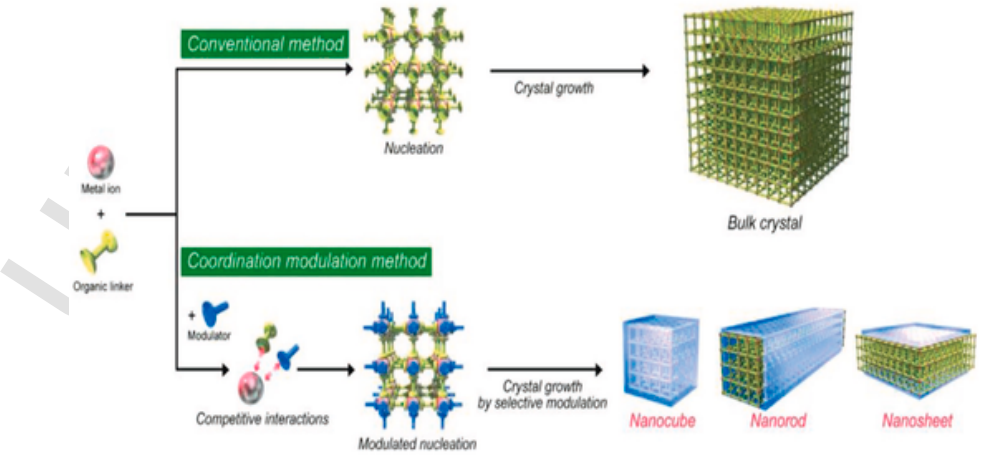

Fig. 2. Coordination modulation method for the preparation of MOF nanocrystals. Reproduced with permission (Tsuruoka et al., 2009). Copyright 2009, Wiley-VCH.

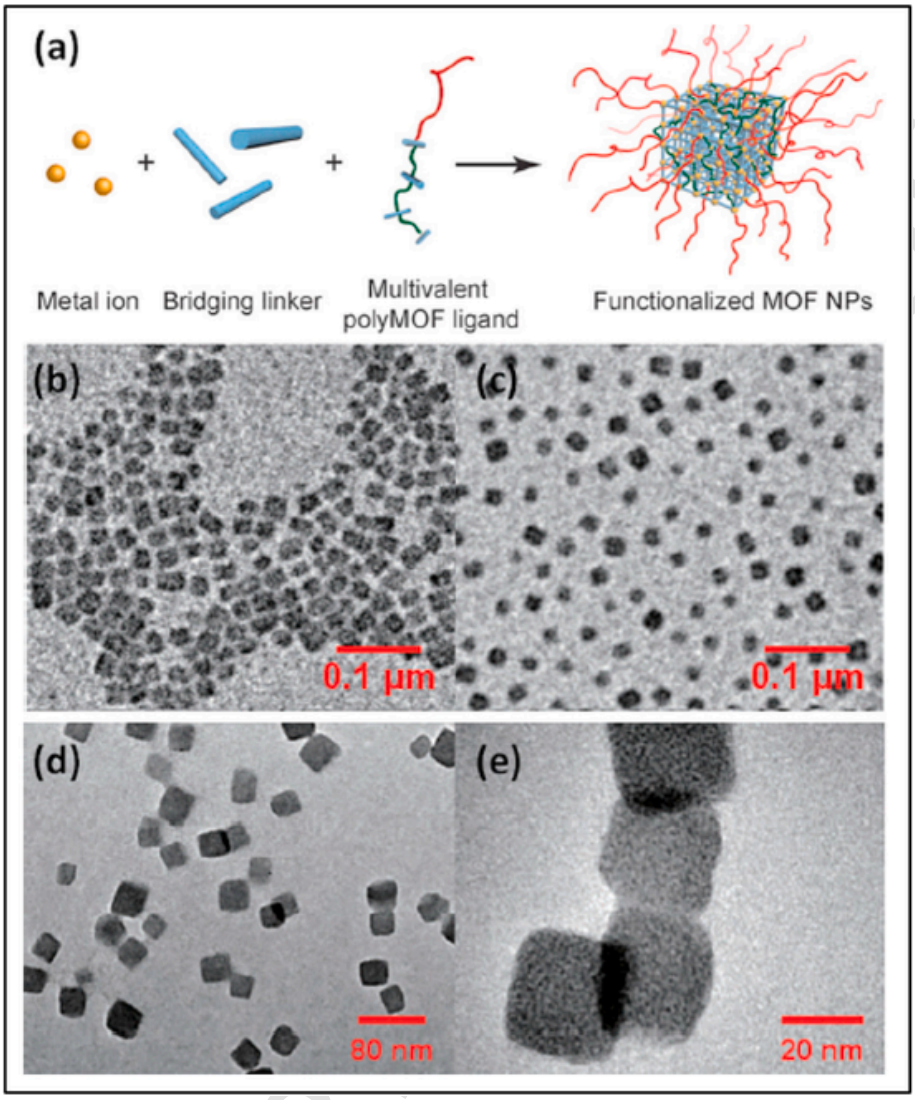

Fig. 3. (a) Formation mechanism of nanosized polyMOFs using multivalent ligands as the modulators. (b) TEM image of the polyMOF-5 nanoparticles with an average diameter of 28 nm synthesized using PEG5k-L_4. (c) TEM image of the polyMOF-5 with an average diameter of 20 nm synthesized using PEG10k-L_4. (d, e) TEM images of the polyUiO-66 with an average diameter of 36 nm synthesized using PEG10k-L_4. Reproduced from reference (Gu et al.,2019) with permission from Wiley-VCH copyright 2019.

ample, by mixing PEG5k-L_4 (PEG10k-L_4 with higher molecular weight), terephthalic acid and zinc nitrate hexahydrate, nanoparticles with an average size of 30 nm (20 nm) were obtained. In another work, Song et al. examined a surfactant-assisted solvothermal synthetic method for the preparation of hollow-structured MIL-125-Titanium (Ti) nanoMOFs (Song et al.,2020;). In this work, they utilized three different types of surfactants: an anionic surfactant, sodium dodecylbenzene sulfonate (SDBS), a cationic surfactant, cetrimonium bromide (CTAB), and a non-ionic surfactant, PVP, to evaluate the effects of different coordination interactions on the morphology and size of MOF nanoparticles. First of all, irregular bulk nanoparticles were obtained without adding surfactants. In the presence of the CTAB surfactant, smaller nanoparticles (dozens of nanometers) along with a small number of thick nano-discs with a thickness of 200 nm were obtained. Also, using SDBS surfactant as the coordination modulator, a large number of spherical nanoparticles were synthesized. Using PVP surfactant gave the best results; uniform hollow-structured nanoparticles with an average diameter of 150 nm were achieved. This phenomenon can be attributed to the different chelating abilities of coordination groups in these surfactants towards Ti^{4+} metal ions. It is well-established that the formation of a reversible metal-ligand coordination is an essential factor in obtaining uniform crystalline nanoparticles. According to this proven rule and given that the coordination interaction between PVP and Ti^{4+} is relatively weak, homogeneous MIL-125-Ti nanospheres were obtained. Overall, by adding surfactants as the coordination modulators, the particle size was decreased, the uniformity was improved, and the morphology was adjusted.

Through extensive research performed on the controllable synthesis of nanoMOFs, nowadays, there is a meaningful understanding over the formation steps of these nanomaterials and recently, some novel synthetic procedures based on the precise segmentation of the nucleation and growth stages are reported to further control the size of nanoMOFs. A generalizable, highly efficient, and scalable strategy for synthesizing a group of nanoMOFs following the aforementioned approach was developed by Zhang et al. (Zhang et al.2019a). In this study, to control the supersaturation degree of the reactants (free monomer concentration), a syringe pump was used to separately supply the metal and ligand and consequently make a balance between supply (followed by immediate nucleation) and consumption (followed by growth of nanoMOFs) of monomers (Fig. 4a). Therefore, there is a dynamic equilibrium between the consumption of the continuously added monomers and the production of nanocrystals all over the process. According to the LaMer's

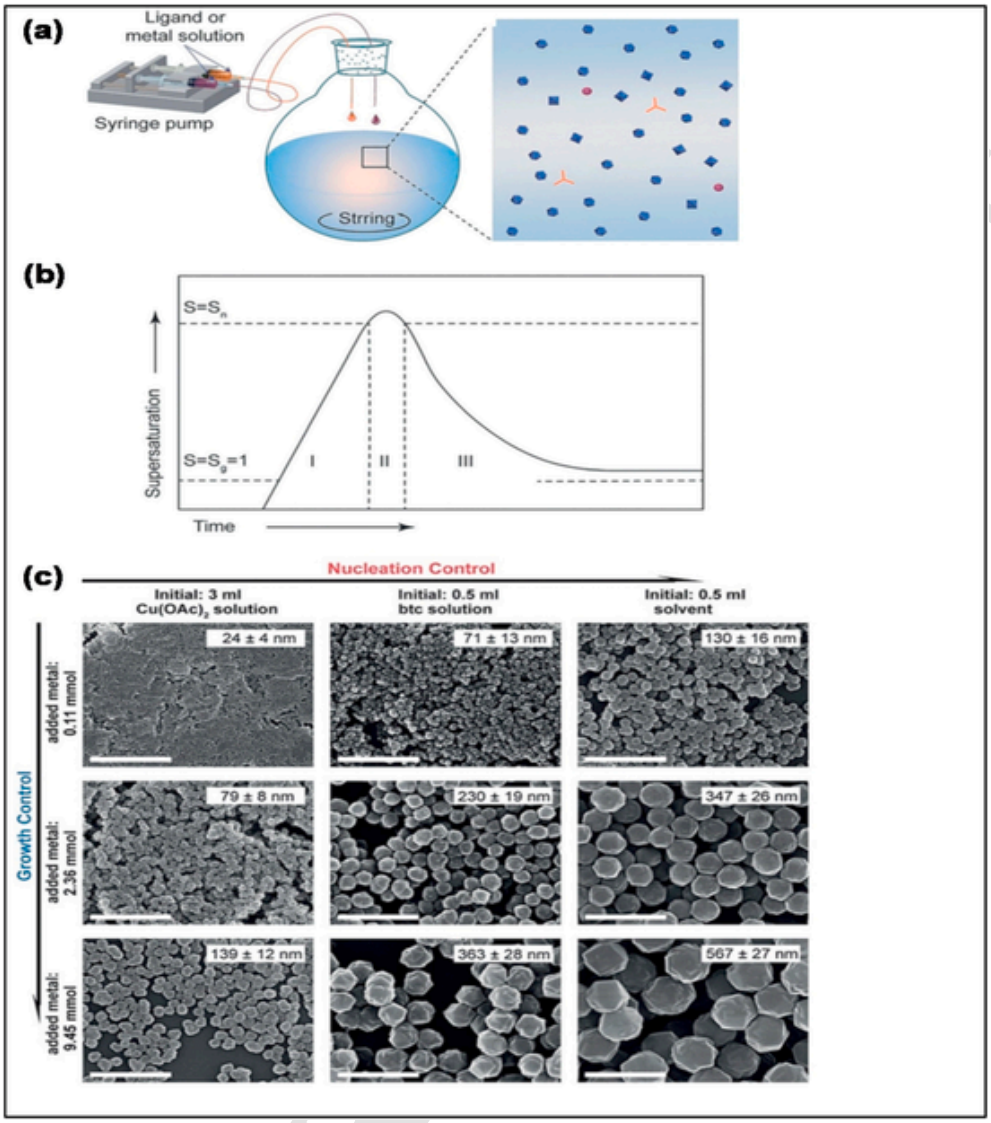

Fig. 4. (a) Schematic view of the synthetic procedure. (b) The LaMer's model diagram. (c) FESEM images of HKUST-1 nanoparticles prepared using different initial solutions after adding different monomers (added metal/ligand = 3/2). Scale bar = 1 μm. Reproduced from reference [Wang et al. 2018] with permission from Wiley-VCH, copyright 2018. 4

model, the supersaturation degree increases initially due to the continuous addition of the reactants (Fig. 4b). On the other hand, this value decreases rapidly due to the quick consumption of monomers during the nuclei growth stage. Afterwards, the totally completed growth of nanocrystals can be obtained by further continuous supply of reactants. By considering the synthesis of nano-HKUST-1 in this study, it was found that the size of nanoparticles was increased by adding reactants. Moreover, the size of products was enhanced by adding a same amount of reactants, when the feed rate at the beginning of the reaction (corresponds to the nucleation) was increased. Since the separation of the nucleation and growth stages is achieved through making a dynamic equilibrium of the reactants' concentrations, the growth of the nanocrystals continues without any considerable agglomeration as long as the amount of reactants is sufficient (Fig. 4c). In other words, by changing the feed rate at the beginning of the reaction, a "controlled nucleation" can be obtained. It is important to mention that this strategy can be developed for the synthesis of various kinds of nanoMOFs such as ZIF-8, ZIF-67, MIL-100(Fe), MIL-101(Fe), MOF-801, and UiO-66-(Zr) which is an evidence that how widely this practical method can be generalized.

2.1.2. Microemulsion method

Microemulsion strategy can be utilized as another effective approach for the fabrication of monodispersed and uniform nanoMOFs. In this method, two incompatible solvents alongside with surfactants or emulsifiers are the main components of the micro emulsion, which is a thermodynamically stable and monodispersed system (Ganguli et al., 2010). Monodispersed droplets can be formed upon the mixing stage and the desired size of droplets can be achieved through addition of sufficient amounts of surfactants. As one of the earlier efforts, the synthesis of Prussian Blue nanoparticles using this method was reported by Mann et al. (Vaucher et al.,2000;). Thereafter, several explorations on the preparation of nanoMOFs through this approach were reported by Lin and co-workers. They synthesized $Gd_2(BDC)_{1.5}(H_2O)_2$ crystalline nanorods using $GdCl_3$ and bis(methylammonium)benzene-1,4-dicarboxylate in a microemulsion system composed of CTAB/water/isooctane/1-hexanol (Rieter et al.,2006;). By changing the water/CTAB ratio from 10:1 to 5:1, the size of nanoMOFs was reduced from 2 μm * 100 nm to 125 nm * 40 nm, which indicates the increase of aspect ratio with the water/surfactant proportion. Moreover, the average size of nanoparticles was decreased by increasing the concentration of reactants. The result could be ascribed to increasing the micelles containing

reactant that provided more nucleation sites and subsequently decreased the size of the nanoparticles. In a similar manner, this reverse-phase microemulsion was extended and used for synthesizing $(Gd(BTC)(H_2O)_2).H_2O$ and $Mn_3(BTC)_2(H_2O)_6$ (Taylor et al.,2008). Very recently, Cai and co-workers prepared highly uniform crystalline nano-HKUST-1 *via* a reverse-phase microemulsion method (Cai et al.,2019b). They first prepared a microemulsion system through adding *n*-hexane, sodium hydroxide solution, and oleic acid (OA) into an ethanol solution of benzene-1,3,5-tricarboxylic acid (BTC). Then, by insertion of the divalent copper ions into the mixture, copper oleate clusters were formed and reacted with the 1, 3,5-benzenetricarboxylicacid (BTC) ligands. Interestingly, the HKUST-1 nanocrystals were slowly formed protected by the OA (Fig. 5a). In this method, it was found that the size of nanocrystals can be controlled by altering the concentration of OA (surfactant) in the mixture. Particularly, by increasing the amount of OA from 0.2 to 0.4 mL while maintaining constant other parameters, the size of nano-HKUST-1 was increased from 30 to 140 nm. Particularly, the uniform nanospheres of HKUST-1 with an average size of 70 nm were obtained by using 0.3 mL of OA in the microemulsion system (Fig. 5b-e). In addition, an iron (III)-based nanoMOF was also synthesized using the same method (Cai et al.,2019c; Cai et al.,2018).

2.2. General Improvement Strategies through Surface Functionalization: Enhancing the Water Stability of Metal-Organic Frameworks

For application in wastewater remediation where contact with water molecules is unavoidable, water stability is a must-have prerequisite in order for MOFs to be viable for use. Early MOFs, such as MOF-5, are reported to be unstable in water (or steam/vapor), as the Zn^{2+} ion is not a high-valence ion that can support strong Zn-O coordination bond (Feng et al.,2018). Recent advancements have led to the creation of thermodynamically water-stable MOFs such as the UiO- and ZIF-series MOFs (Lee et al.,2018). In general, the water stability of these MOFs can be attributed to its metal-ligand coordination bond, which is stronger than the bond between the MOF's metal center and water molecules, thus preventing water from taking over and hydrolyzing the bond. This can be achieved by using high-valence metal ions (e.g., Zr, Ce) instead of lower valence ions (e.g., Zn, Cu) (Burtch et al.,2014). While the aforementioned criteria are necessary to enhance the MOF's thermodynamic stability, it is not the sole governing factor of the MOF's stability in water. Another aspect to consider is kinetic stability, which can be achieved by relying on sufficiently high activation energy barrier (Ea) being present (Nguyen and Cohen.,2010). Thus, even if a MOF does not possess inherently good thermodynamic stability (i.e., water could hydrolyze the coordination bond if it manages to reach the metal core), stability may still be achieved by kinetic factors that pro-

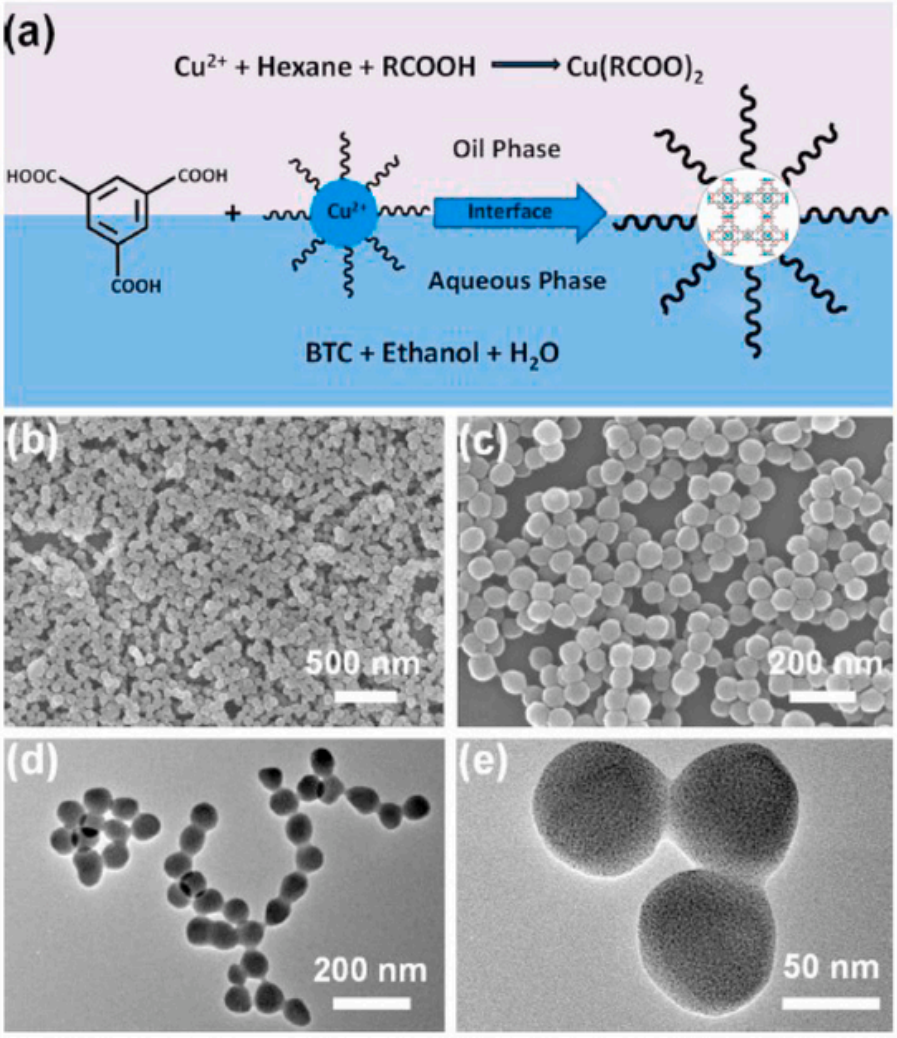

Fig. 5. (a) Schematic diagram of the synthetic mechanism of HKUST-1 nanocrystals. SEM (b, c) and TEM (d, e) images of nano HKUST-1 at different magnifications. Reproduced from ref (Cai et al.,2019b). with permission from the American Chemical Society, copyright 2019.

vide high activation energy barrier (i.e., the water could not even come near the metal core), including steric effects and hydrophobicity. In the former case, high metal coordination numbers can create a crowding effect, as well as the presence of ligands with aromatic structure that generate steric hindrance. In the latter case, hydrophobicity itself can be divided into two criteria: (1) hydrophobicity in the MOF's internal structure, and (2) hydrophobicity in the surface/pores. As this review aims to mainly discuss the improvement strategies on existing MOFs in wastewater remediation, strategies that involve changing the internal MOF's structure/component during synthesis (i.e., thermodynamic stability) will not be discussed. A comprehensive review and compilation discussing the relation between each of the MOF's structural factors and its water stability has been elegantly published by Burtch et al. (Burtch et al.,2014). This section of the review will mainly focus on discussing the post-synthesis modification of existing MOF structure to make it more water-stable, which includes surface hydrophobic modification, as well as ligand functionalization and introducing hydrophobic coating. A summary of strategies for improvement of water-stability of MOFs is presented in Fig. 6.

2. 2. 1. Ligand Functionalization

There are two ways in which the functionalization of ligands can improve the water stability of a given MOF. The first mechanism is by improving the internal hydrophobicity of the MOF. It has been widely reported that MOFs stability in water can be improved by incorporating hydrophobic fluorinated and alkyl functional groups on the organic ligands. The presence of a bulky and long alkyl group was proven to turn IRMOF-3, which is not inherently hydrophobic, into a hydrophobic material (Drache et al.,2016). Additionally, the modification of aminated MIL-53 (MIL-53(Al)–NH_2) by alkyl anhydrides through amide bond formation generated a superhydrophobic material. Another mechanism in which ligand functionalization can improve the water stability is through steric factors. An interesting MOF to discuss here is UiO-66, where the MOF contains carboxylate ligands that have low pKa, and thus are susceptible to hydrolysis. The stability of UiO-66 can be attributed to two factors. The first one is due to the high coordination number, which creates a crowding effect and prevents water from clustering near the metal core. The second one can be ascribed to the ligand itself, where the aromatic rings in the UiO-66 can exhibit significant rotational dynamics. DeCoste et al. demonstrated that UiO-67, which contains two aromatic rings, is more susceptible to water than UiO-66 with only one aromatic ring, possibly due to the greater torsional strain created around the metal cluster (Li et al.,2021a,b). Based on those principles, Zhang et al. developed a new highly water stable Zr-based MOF (DeCoste et al.,2013). The group designed new Zr-based MOFs with hexacarboxylate ligands as functional groups, and the metal clusters are modified with four different functional groups, including $HCOO^-$, CH_3COO^-, H_2O/OH and $PhCOO^-$.

2.2. 2. Addition of Hydrophobic Coating

The other strategy to improve the water stability of MOFs is through introducing hydrophobic molecules/polymers as hydrophobic coatings to increase surface hydrophobicity of the MOF. Sun et al. successfully introduced a hydrophobic octadecyl phosphonic acid (OPA) layer onto the surface of several Zr-based MOFs (UiO-66, UiO-66-SO_3H, PCN-222) through immersion in OPA ethanol solution for 24 h (Zhang et al., 2018). Addition of OPA coating on the surface of Zr-based MOFs boosted the MOF's hydrophobicity from hydrophilic pristine MOFs (water contact angle (WCA) of UiO-66, UiO-66-SO_3H and PCN-222 were 19°, 10°, and 15°, respectively) to superhydrophobic OPA-coated MOFs (WCA of OPA-UiO-66, OPA-UiO-66-SO3H and OPA-PCN-222 were 160°, 162°, and 157°, respectively). The water stability of OPA-UiO-66-SO_3H and OPA-PCN-222 was tested by immersing the MOFs in basic aqueous solution (pH = 11) for seven days. The water stability test was conducted only in basic solution as previous study reported that the MOFs were stable in acidic solutions (Batra et al.,2020; Sun et al.,2017). Both OPA-UiO-66-SO_3H and OPA-PCN-222 retained their respective surface area of 1156 and 1713 m^2/g after seven days, while under the same conditions pristine UiO-66-SO_3H lost 53.8% of its surface area (decrease from 1156 to 534 m^2/g) and pristine PCN-222 completely dissolved into the solution. Qian et al. treated DUT-4 with organosilicon (namely hydrophobic-treated (HT) DUT-4) by immersing the MOF in an organosilicon heptane solution and found that the MOF's WCA was significantly increased from 13 ± 2° (pristine DUT-4) to 148 ± 3° (HT DUT-4) (Juan-Alcañiz et al.,2013). Water stability of the pristine and HT DUT-4 was evaluated in acidic, neutral, and basic aqueous solutions at 50 °C for six days. The surface area of the pristine DUT-4 decreased by about 80% from 1183.8 m^2/g to 192.7, 224.5, and 206.8 m^2/g after six days' immersion in acidic, neutral, and basic solution, respectively. On the other hand, HT DUT-4 retained around 80% of its initial surface area (1125.4 m^2/g) in acidic, neutral, and basic solutions after six days with a surface area of 903.6, 983.8, and 935.4 m^2/g, respectively. In addition of using hydrophobic molecules, several studies successfully increased the surface hydrophobicity of MOFs by introducing hydrophobic polymeric materials onto the MOFs. Ding et al.2020 increased hydrophobicity and water stability of HKUST-1 by creating hydrophobic layer of polydimethylsiloxane (PDMS) on the MOF surface through post synthesis *in-situ* polymerization (Feng et al.,2012).

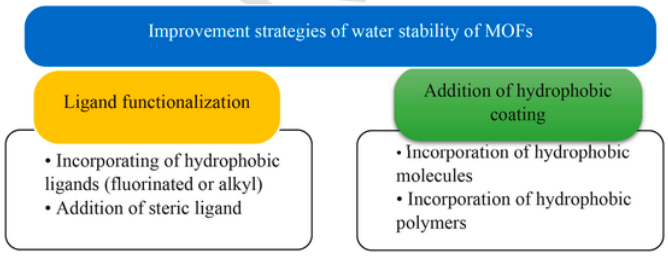

Fig. 6. Improvement strategies of water-stability of MOFs through post-synthesis modification.

3. Specific Improvement Strategies Related to Metal-Organic Frameworks in Wastewater Treatment

3.1. Metal-Organic Frameworks as Adsorbents

Adsorption is an attractive method to remove pollutants from wastewater due to its simplicity and relatively low cost (Qian et al.,2019). The most commonly used adsorbents for wastewater pollutants' removal is activated carbon (AC) (Ding and Jiang,2020). AC is popular due to its high surface area (up to 1100 m^2/g) and high pore volume (up to 0.40 m^3/g) (Yi et al.,2021), which facilitate effective adsorption of pollutants (up to 50% of initial concentration) (Bernal et al.,2021,2020, 2018; Crini et al.,2019; Seow et al., 2016). However, the ideal adsorbents should not only exhibit high adsorption capacity, but also high adsorption selectivity of the persistent organic pollutants (95,96). In this context, MOFs are promising alternative adsorbents due to their extraordinary high surface area (up to 7000 m^2/g), high adsorption capacity, ability to bind various organic pollutants, and adsorption selectivity (De Franco et al.,2018; SaÖzdemir and Önal, 2018; Zimpel et al., 2016). it was shown that MIL-101(Cr) has higher methyl orange (MO) adsorption capacity (114.0 mg/g) than AC (11.2 mg/g), due to significantly higher surface area of MIL-101(Cr) (3873 m^2/g) compared to AC (1068 m^2/g) (Kårelid et al.,2017). MOFs also exhibit good adsorption capacity for other emerging pollutants such as antibiotics and polycyclic aromatic hydrocarbons (PAHs). In a study by Chen et al. (Chen et al.2018; Zango et al.,2020), UiO-66 revealed significantly higher adsorption capacity for tetracycline hydrochloride (TH; 23.1 mg/g) antibiotics compared to the adsorption capacity of AC for the same substance (1.98 mg/g) previously re-

ported (Au,2020). In a report by Zango et al. (Zango et al.,2020; Haque et al.2011), MIL-88(Fe) achieved an adsorption capacity of 23.6 mg/g for the highly toxic PAH anthracene (ANT), performing better than AC with an adsorption capacity of 8.35 mg/g (Chen et al.2018). Several other reports of MOF application as adsorbents of wastewater emerging pollutants and their adsorptive performance are listed in Table 1. In this section, three strategies to further improve the performance of water-stable MOFs as adsorbents of wastewater pollutants will be discussed. These methods are based on functionalization, metal doping, and MOF-polymer composites.

3.1.1. Effect of Functionalization

In most cases, MOFs adsorb organic pollutants through various types of interactions. Thus, MOFs' functionalization by incorporating additional organic groups such as -NH_2, -COOH, or -SO_3H could improve their adsorption capacity by providing additional interactions through electrostatic attraction and/or hydrogen bonding (Chalati et al., 2011; Chen et al., 2019a; Cravillon et al., 2009; Hermes et al., 2007; Lai et al.,2015; Pouretedal and Sadegh, 2014; El Khames Saad et al., 2014; Zango et al., 2019). Furthermore, ligand functionalization of MOFs could also enhance their adsorption capacity, selectivity, stability, and reusability. Sulfonic acid (-SO_3H) functionalization of MOF is effective to improve its adsorption capacity for anionic organic pollutants through electrostatic interactions since sulfonic acid functional groups could increase the positive charge of the MOF. Yang et al. found a significant improvement of adsorption capacity of sulfonic acid MIL-101(Cr) (MIL- 101-SO_3H) for anionic synthetic dyes, such as MO and Congo red (CR) (Cai et al.,2016). They observed that MO adsorption capacity of MIL-101-SO_3H (688.9 mg/g) is 1.7 times higher than that of pristine MIL-101(Cr) (406.1 mg/g). While CR adsorption capacity of MIL-101-SO_3H (2592.7 mg/g) is 1.9 times higher than that of its pristine form (1367.1 mg/g). An anomaly phenomenon was observed on the adsorption capability of MIL-101-SO_3H for acid chrome blue K (ACK) dye. Even though ACK is also a negatively charged dye molecule, its nonlinear structure hinders the interactions between the MOFs and the dye. As a consequence, the ACK adsorption capacity of MIL-101-SO_3H (213.2 mg/g) is 0.7 times lower than its pristine form (323.1 mg/g). Amination (addition of amine functional group) is one of the most studied MOFs' functionalization strategies and demonstrated fascinating features. Not only it could enhance MOFs adsorption capacity by providing an extra interaction through hydrogen bonding and/or electrostatic interaction, but also it could control MOFs' adsorption capacity and selectivity by tuning their pH (Gao et al., 2020; He et al., 2017, Kårelid et al., 2017). Lv et al. 2019 showed that the introduction of amine group could increase the adsorption capacity of UiO-66 by about 150% and adsorption capacity and selectivity of the aminated MOF (UiO-66-NH_2) was strongly affected by pH (Kårelid et al., 2017). In acidic condition, UiO-66-NH_2 tends to adsorb anionic MO through electrostatic interaction, because the positive surface charge of the MOF was formed in acidic condition as the result of amine protonation. On the contrary, adsorption of cationic MB is preferable ~~at~~ basic conditions through electrostatic interaction due to the presence of the negatively charged UiO-66-NH_2. Interestingly, amination could also enhance MOFs' adsorption capacity for both MO and MB at neutral condition by providing additional hydrogen bonds between the MOF and the dyes. Schematic illustration of the adsorption mechanism of the aminated MOF for anionic MO and cationic MB at various pH can be seen in Fig. 7.

Zhuang et al. used similar aminated MOF (UiO-66-NH_2) for anionic diclofenac (DCF) adsorption and they found that the DCF adsorption capacity of the aminated MOF (555 mg/g) is 1.5 times higher than that of its pristine MOF (357 mg/g). Amine groups in UiO-66-NH_2 increased its adsorption capacity by acting as DCF adsorption sites through hydrogen bonding and positively charges of the aminated MOFs are favorable for anionic DCF adsorption through electrostatic interaction. The effect of amination on elevating the adsorption capacity of MOFs was also observed on other MOFs and different organic pollutants. Park et al. reported that amination of MIL-101(Cr) led to 260% improvement for bisphenol S (BPS) adsorption capacity, from 196 mg/g (pristine MOF) to 513 mg/g (aminated MOFs), owing to the hydrogen bonding between BPS and amine groups (Ayala et al.,2019; Pouretedal and Sadegh, 2014). An incredible improvement of the MOFs' adsorption capacity for cationic pollutants could be attained by carboxyl functionalization (Gao et al.2019,2020). demonstrated that the carboxyl-functionalized UiO-66 and UiO-66-$(COOH)_2$ could achieve ultra-high adsorption of Rhodamine B (RhB) with a maximum adsorption capacity of 2200 mg/g at high RhB concentration, which is 11 times higher than its pristine form (200.4 mg/g) (Boles et al.,2016). Carboxyl functionalization increased the RhB adsorption of UiO-66 by altering the surface charge of the MOF. The surface of UiO-66 is positively charged in acidic pH, while the surface of UiO-66-$(COOH)_2$ is strongly negatively charged, enhancing the adsorption of the MOF for cationic pollutants such as RhB. Other MOF functionalization with -OH, -NO_2, and -Br groups could also enhance MOFs' adsorption capacity. Hydroxyl functionalization could improve the adsorption capacity of MIL-101(Cr) for various organic pollutants by providing an additional hydrogen bonding between -OH group and organic pollutant (He et al., 2017). ~~While~~ -NO_2 and -Br functionalization could enrich TC adsorption capacity of MIL-53(Fe) by increasing its positive charge, leading to improvement of electrostatic attraction between the MOF and TC (Gao et al., 2020). The

Table 1
Examples of MOFs utilization as adsorbents for persistent organic pollutants (POPs).

MOF	Surface Area (m^2/g)	Target Pollutant	Pollutant Concentration	Adsorption Conditions	Adsorption Capacity (mg/g)	Reusability (Cycles)	Ref.
MIL-101 (Cr)	2410	Reactive Yellow 15 Reactive Black 5 Reactive Red 24 Reactive Blue 2	300 ppm	30 °C, pH 7, 24 h	397 386 390 377	4	(Haque et al.2011)
	2710	2-chlorophenol	300 ppm	25 °C, 24 h	121	-	(Gu et al.,2019)
MIL-88(Fe)	1240	Anthracene	4 ppm	25 °C, pH 2-6, 25 min	23.6		(Au,2020)
UiO-66	1276	Methyl Red Methyl Orange Malachite Green Methylene Blue	200 ppm	25 °C, pH 5.5, 120 min	384 454 133 370	4	(Chen et al.2018)
	591.6	Tetracycline Hydrochloride	100 ppm		23.1	-	(Kårelid et al.2017)
UiO-67	2345	Atrazine	6 mg/L	25 °C, 24 h	17.5	3	(Chen et al.2018)
ZIF-8	1875	Atrazine			8.9		
CaFu-MOF	2308	Imidacloprid	0.1 mmol/L	25 °C, PH 6.5, 70 min	467.2	5	(Wang et al., 2018b)

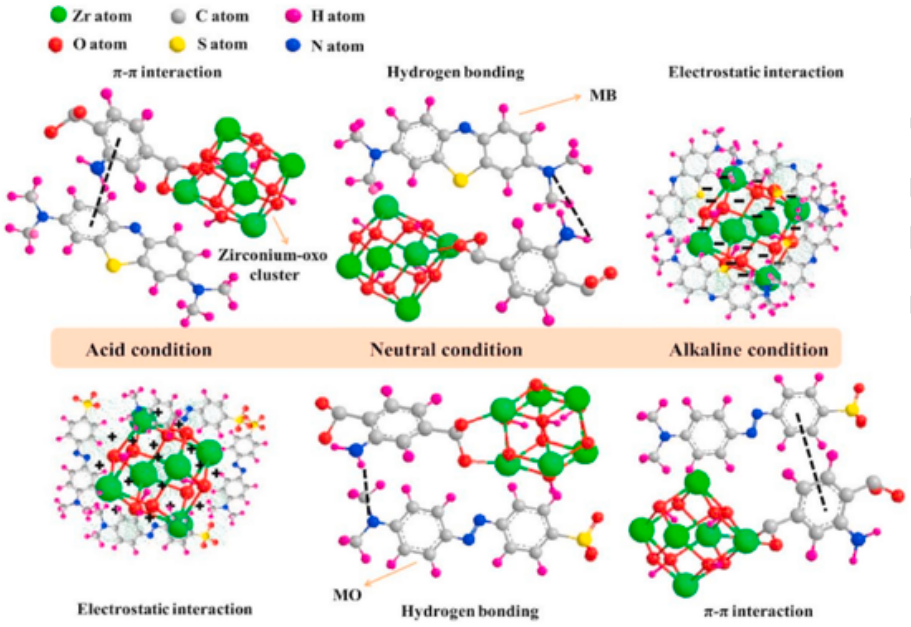

Fig. 7. Schematic illustration of adsorption mechanism of the aminated MOF for the anionic MO and cationic MB at various pH. Reproduced with permission from ref (lv et al.,2019). Copyright (2019) Elsevier.

effects of functionalization on adsorption capacity of the MOFs are summarized in Table 2.

3.1.2. *Influence of Metal Doping*

The addition of metal atoms may affect the charge of the MOFs and subsequently enhance the electrostatic attraction between the MOFs and pollutants. In a report by Yang et al., the effect of cerium (Ce) doping of UiO-66 on the dye adsorption capabilities for MB, MO, CR, and ACK was assessed. Ce-doped UiO-66 featured a larger surface area of 1135 m^2/g compared to pristine UiO-66 (981 m^2/g) (McGuire et al., 2015). The Ce-doped UiO-66 achieved adsorption capacities of 145.3, 639.7, 826.7, and 245.8 mg/g for MB, MO, CR, and ACK, respectively, higher than pristine UiO-66 (24.5, 172.5, 495.0, and 230.9 mg/g, respectively). The increase of MB adsorption on the Ce-doped UiO-66 was due to the decrease of positive charge, following Ce doping, which reduces the repulsion between the MOF and the cationic MB. The enhanced adsorption of anionic dyes MO and CR, despite the decrease of the positive surface charge of the MOF, was ascribed to Ce particles serving as additional active sites on the MOF, which adsorb the dyes through π-π interactions. The adsorption of ACK on Ce-doped UiO-66 did not increase, presumably due to the non-linear structure of ACK molecule which hindered the interactions between the ACK dye and Ce sites, preventing additional dye adsorption by the Ce particles. Zhang et al. reported the effect of Fe-doping on the adsorption capability of Zr-based MOF for MB and MO (Alexis et al., 2008). The Fe-doped MOF-545, or Fe-loaded MOF-545(Fe) displayed lower adsorption capacity for MB and higher adsorption for MO compared to the undoped MOF-545. The Fe-loaded MOF-545(Fe) adsorption capacities were 382.35 and

Table 2
The influence of functionalization on adsorption capacity of MO Fs.

Functionalization	MOF	Target Pollutant	Adsorption Capacity			Reusability	Ref.
			Pristine MOF (mg/g)	Functionalized MOF (mg/g)	Improvement (%)		
Sulfonation	MIL-101-SO_3H	Methyl Orange	406.1	688.9	169.6	5 cycles, 88%	(Murray et al., 2000)
		Congo Red	1367.1	2592.7	189.6		
		Acid Chrome K	323.1	213.2	66.0		
Amination	UiO-66-NH_2	Methyl Orange	107.9	148.4	137.5	6 cycles,	(Chen et al.,2019b)
		Methylene Blue	392.6	549.6	140.0	86.2% (MO), 88.2% (MB)	
		Diclofenac	357	555	155.5	Not reported	(McGuire et al., 2015)
	MIL-53 (Al-BDC)	Dimethoate	154.8	513.4 (Al-$(BDC)_{0.5}$ $BDC\text{-}NH_2)_{0.5}$)) 266.9 (Al-(BDC-NH_2))	331.7 172.4	Not reported	(He et al., 2017)
	MIL-101- NH_2	Bisphenol S	196	513	261.7	5 cycles, 90%	(Ayala et al.,2019)
	NH_2-MIL-53(Fe)	Tetracycline	248.3	271.8	109.5	4 cycles, 80%	(Boles et al.,2016)
Carboxylation	UiO-66-$(COOH)_2$	Rhodamine B	200.4	2200	1097.8	6 cycles, 73%	(Chen et al.,2019b)
Hydroxylation	MIL-101-$(OH)_3$	P-Chloro-m-Xylenol	64	79	123.4	Not reported	(Murray et al., 2000)
		Bisphenol A	73	97	132.9		
		Triclosan	79	112	141.8		
		Ketoprofen	48	80	166.7		
		Naproxen	88	156	172.3		
Nitro Functionalization	NO-MIL-53(Fe)	Tetracycline	248.3	272.6	109.8	4 cycles, 80%	(Ayala et al.,2019)
Bromination	Br-MIL-53(Fe)	Tetracycline	248.3	309.6	124.7	4 cycles, 80%	(Ayala et al.,2019)

803.664 mg/g for MB and MO, respectively, while the undoped MOF-545 exhibited adsorption capacities of 906 and 589 mg/g for MB and MO, respectively. The decrease of MB adsorption capacity was due to the increase of the positive surface charge of the MOF following Fe doping, which also resulted in better attraction and adsorption of MO. The effect of Mn doping on the adsorption capability of UiO- 66 for tetracycline (TC) was reported (Wang et al., 2018a,b). The maximum adsorption capacity of the Mn-doped UiO-66 (Mn-UiO-66) for TC was 184.49 mg/g, higher than the maximum TC adsorption capacity of pristine UiO-66 (23.1 mg/g). Mn doping increased the amount of adsorption active sites on the MOF through donation of valence electrons, resulting in enhanced adsorption capacity of the MOF. The Mn-UiO-66 also showed good reusability, retaining 84% of its initial adsorption capacity after three cycles. Sun et al. (Sun et al., 2017) reported the effect of Cu doping on the adsorption capability of ZIF-8 for TC. The reported maximum TC adsorption capacity of the Cu-doped ZIF-8 (Cu-ZIF-8) was 307.9 mg/g, 2.4 times higher than that of pristine ZIF-8. The Cu-doping increased the adsorption capacity of ZIF-8 by donating valence electrons to the MOF. Cu-ZIF-8 also revealed very good stability in water and reusability. The adsorption capacity of Cu-ZIF-8 sample decreased to 139.8 mg/g from the initial capacity of 156.5 mg/g after four cycles.

3.1.3. MOF-Polymer Composites

MOF can be combined with polymers to create MOF-polymer composites. This way, the MOF's porosity can be enhanced, new functionalities can be imbued, and its stability can be improved (Nakajima et al., 1995). The composite can be formed by *in situ* polymerization inside the MOF's pores, constructed either by polymeric ligands, introduced by post-synthesis (covalent grafting or incorporating separately the polymer), or self-assembly of MOFs on pre-synthesized polymers. Rather than enhancing the adsorptive capability of the MOF, the creation of MOF-polymer composites often aims to ease the process of recovery and separation, as well as improving the stability of the MOF itself without compromising the performance. Several MOFs are known to exhibit poor stability in aqueous media due to the presence of species (e.g., H_2O, H^+, OH^-), which can hydrolyze the metal or protonate the ligands. This can be largely remediated by grafting polymers onto the MOF's surface, as was demonstrated by Hou et al. (Hou et al., 2016; Shih et al., 2012). Polymethylmethacrylate (PMMA) was grafted onto UiO-66-NH_2 by soaking the MOF into a solvent containing MMA monomers, followed by UV irradiation, forming polymer brushes on the surface of the MOF. The presence of the polymer brushes was found to be able to enhance the MOF's chemical and thermal stabilities, without significantly decreasing the porosity and surface area for adsorption. As with many reports on MOF-polymer composites, a decrease in BET surface area is expected as a compromise for significantly enhanced stability. Nevertheless, the presence of flexible grafted polymers on the MOF's surface may help to compensate partially the loss of the surface area in terms of adsorption performance by filling the gaps between the MOF's particle and promote pollutant transport *via* the MOF's pores. As such, the presence of grafted polymer was able to enhance the removal efficiency of R-250 dye despite the loss in surface area. To enhance reusability and facilitate separation after usage, Abdi and Abedini prepared polyether sulfone (PES)-ZIF-8/ZIF-67 nanocomposite in the form of beads, using a one-step phase inversion method (Abdi and Abedini, 2020; Ling et al., 2015). The addition of MOF significantly improved the polymer's BET surface area and total pore volume, even though it is still lower than pristine ZIF-8 and ZIF-67. The nanocomposite exhibited low adsorption capacity at extremely low pH due to the repulsive electrostatic interaction between ZIF and malachite green, but gradually improved when the pH was increased due to stacking interaction.

3.2. Metal-Organic Frameworks as Catalysts in Catalytic Degradation of Wastewater Pollutants

As previously discussed, the MOF' general advantages as a catalyst means that the material has a huge potential to outperform the conventional photocatalysts, as well as conventional Fenton or Fenton-like catalysts. Nevertheless, improvements must be made to address their current weaknesses and make them viable for practical applications. Recently, mixed-metal MOF systems, consisting of MOFs comprising two or more metal ions as nodes in the same MOF phase, have demonstrated excellent results in MOF-based catalysis (Karagiaridi et al., 2014). This is usually achieved by doping metal ions into existing MOF (the strategy will be discussed in more detail below). Alternatively, combining two materials to create a composite system has been receiving major attention in catalysis. In this scenario, one material will act as a structural support for anchoring the catalytically active second material in order to enhance its stability and ensuring reusability (Zhang et al.,2014). Huge efforts to combine MOFs with other functional materials which can be confined inside the MOFs' structure thanks to its permanent porosity with the aim to enhance their catalytic properties have been attempted (Karagiaridi et al., 2014; Ma et al.,2017; Sorribas et al., 2013). Among these, the addition of other catalytically active materials as guest species have been demonstrated, and the combinations are generally reported to be synergistic and successful in increasing the MOFs' catalytic activity to degrade various organic pollutants found in wastewater. The combination of MOFs and other nanostructured materials including metal nanoparticles (MNPs), semiconductors, and nanostructured carbon (e.g., graphene, carbon nanotubes) represents an interesting topic in the field of catalysis and generated a huge interest in recent years. Such nanostructures are known to possess high surface energy. Therefore, they are prone to aggregation, which will lead to a decrease in catalytic performance. On the other hand, being a porous structure, MOFs have the potential to facilitate other catalytically active guest species to enhance its overall catalytic performance. When combined, the MOFs act as a spatial confinement to the guest species, preventing them from aggregating with each other, while still allowing for substrate transport. The catalytically active guest species, in turn, will elevate the MOFs' catalytic activity—which is often meager on its own—by creating a composite alongside the MOF. The MOFs may act as a mere host for the guest species, or it can also participate in the catalysis process as a co-catalyst.

This section of this review will highlight the basic concepts of enhancement *via* doping and/or creation of nanocomposites with metal, semiconductors, and carbon-based materials, as well as providing examples of recent advances in MOFs-based photocatalysis in wastewater remediation.

Influence of Metal Addition. Metals can be used as dopants to create mixed-metal MOF systems or in the form of separate metal nanoparticles (MNPs) to create a nanocomposite with the MOFs. This holds true for both photocatalysis and Fenton-like catalysis alike. An example of metal doping was demonstrated by Avilés et al., who reported Zr doping of NH_2-MIL-125(Ti) with a specific molar ratio, aimed for degradation of acetaminophen under solar light irradiation (Aviles et al.,2019; Bedia et al., 2019; Xiao et al.,2019). Zr doping is known to be able to increase the photocatalytic activity of TiO_2 due to the lower energy band gap value, while NH_2-MIL-125(Ti) is chosen due to its large surface area and satisfactory stability. The addition of Zr is meant to substitute some of the Ti content in the MOF, and indeed changes in the MOF's crystal structure were observed by varying the Ti:Zr molar ratio. Nevertheless, when the Zr concentrations are too high, the MOF structure was found to be amorphous, leading to reduction in catalytic activity. In a similar manner, doping of Cu onto NH_2-MIL-125(Ti) was also reported to enhance its photocatalytic activity (Wang et al.,2015). Cu was chosen as it is more electronegative than Ti, while having similar ionic radius, thus resulting in good doping efficiency. In agreement with the previous re-

port, excessive doping of Cu leads to a decrease in photocatalytic activity due to formation of defects, which may function as recombination centers for the photogenerated carriers. Even though metal doping may not necessarily enhance the surface area of the MOFs (or in this case, even slightly reduced), increase in photocatalytic activity is often achieved through other means; it is usually attributed to more efficient charge separation and charge transfer efficiency or improved light absorption ability. Another example was recently demonstrated by Wang et al., who doped Fe(III) onto NH_2-MIL-68(In) for visible-light-driven photocatalytic reduction of Cr(VI) and degradation of tetracycline hydrochloride (TC-HCl) (Bonnett et al.,2020). Notably, the group had previously synthesized Ag NPs loaded onto NH_2-UiO-66 and reported significant improvement in performance, but aggregation of Ag NPs was also reported ~~to some extent~~ (Seyedpour et al., 2019). In order to prevent aggregation and to further boost the efficiency of noble metal catalyst for the case of MNPs/MOFs composites, many contemporary demonstrations developed various strategies to improve their activity by creating unique architectural nanostructures such as core-shell/yolk-shell structures, or combining the MNPs with other materials such as metal oxides or carbon-based materials. Both of these were elegantly demonstrated by Tilgner et al.,2017 who reported the fabrication of MIL-101(Cr) core with Au/TiO_2 anatase shell as visible-light-driven photocatalyst ~~of~~ rhodamine B as a model dye (trilgner et al.2017; Liu et al.,2011). Addition of precious metals (e.g., Au, Pd, Pt) into MOFs is able to inhibit the photogenerated electron-hole recombination due to the formation of Schottky barrier at the junction between MOFs and the metal, leading to more efficient charge carriers' separation of the catalyst system. Thus, they will practically translate into better photocatalytic performance (Liu et al., 2017b; Wibowo et al., 2021).

4. Fabrication strategies of different kinds of nanoMOF-based membranes

With improvements of the various rational fabrication strategies of nanoMOF-based membranes over the past decade, the applications of these membranes for water-treatment have gotten more and more prominent. A summary of various strategies of making nanoMOF-based composite membranes is presented in Table 3. A well-designed nanoMOF-based membrane has to be a perfect combination of nanoMOF synthesis (comprehensively discussed in the previous section) and membrane fabrication. Different strategies for fabricating nanoMOF-based membranes have been devised and reported. Among them, thin-film nanocomposite (TFN) and mixed-matrix membranes (MMMs) as the most common and efficient methods due to the unique physiochemical properties of the produced membranes, will be discussed in-depth. However, there are some less-used methods that will be also discussed in this part to provide a broader idea for the reader.

4.1. Thin-film nanocomposite (TFN) membranes

The TFN membranes are composed of a polymeric support layer (SL) with high porosity and relatively high thickness, which is responsible for the membrane mechanical strength, and an ultra-thin active layer (AL) responsible for the separation ability (Zirehpour et al. 2017). The AL is mostly made of polyamide (PA), which is formed on the SL by a chemical reaction named interfacial polymerization (IP) between two monomers (commonly trimesoyl chloride (TMC) & *m*-phenylenediamine (MPD)) dissolved in two different solutions (organic and aqueous, respectively), individually (Fig. 8a) (Zirehpour et al. 2017; Zhao et al.,2019a). This highly cross-linked and ultra-thin layer is responsible for the rejection of pollutants and separation performance in general meaning. The SL can be fabricated by different methods, even though the phase inversion (PI) method is the most prominent one in which a polymeric solution (polymer dissolved in an organic solvent) is casted on a plate (e.g. glass plate) and then immediately immersed in a water bath for solvent/dissolvent (water) exchange, and a membrane sheet is obtained after a day (Lau et al., 2015). This highly porous and thick layer is responsible for the membrane mechanical resistance. Indeed, the correct term for as-mentioned membrane is thin-film composite (TFC) membrane, which by incorporating the MOF nanoparticles into the structure of AL, a complete TFN membrane is fabricated (Fig. 8b) (Gu et al., 2019b). MOF was firstly added into a TFN membrane as a filler by Sorribas et al. (Sorribas et al. 2013). Because of the nanoscale particle sizes, identical pore sizes, and reticulated porous structures, the resulting membrane showed better appetency with polymer chains than other types of nanoparticles (Huang et al., 2020). Zeyedpour and co-workers fabricated a TFN-forward osmosis (FO) membrane with an AL incorporated with silver-based MOF nanoparticles to enhance the water permeability (Seyedpour et al 2020 a,b). The MOF nanoparticles were firstly synthesized using silver (I) and 1,3,5-benzene tricarboxylic acid (3HBTC). To form an AL on the SL, made of polyethersulfone (PES), the aforementioned IP reaction between MPD and TMC was performed, except that in this method they dispersed the MOF nanoparticles in the or-

Table 3
Various strategies ~~of making~~ nanoMOF-based composite membranes with a brief description of their unique characteristics.

Membrane type	Strategy	Unique characteristics	Ref.
TFN	Incorporating the MOF nanoparticles into the PA layer through the IP process	There is possibility to change the properties of the PA layer such as cross-linking degree and thickness, hence increasing the water permeance, and rejection ability in some cases	(Arjmandi et al., 2019a)
	Coating a layer of nanoMOFs on the PA layer through direct coating or surface growth	There is possibility to change the membrane surface hydrophilicity and charge, hence introducing or improving the antifouling and antibacterial properties, leading to the long-lasting membranes with high separation efficiency	(Liu et al., 2019 b)
MMM	Incorporating the MOF nanoparticles into the substrate or single-layer membrane through the PI process	There is a possibility to increase the porosity and decrease the membrane thickness and tortuosity, leading to a decreased S-value and increased water flux	(Arjmandi et al., 2020b Arjmandi et al., 2019b; Chen et al., 2016; Seyedpour et al., 2018)
Others	PMM; Using the water-unstable MOF nanoparticles as the pore formers	There is a possibility to increase the membrane porosity and regulate the mean pore size through adjusting the size of nanoparticles, without affecting the membrane chemical properties such as hydrophilicity and surface charge	(Ding et al. 2014)
	Forming a selective layer of nanoMOFs on the substrate through different approaches such as electrochemically-assisted interfacial growth, phase transformation interfacial growth, pressure-assisted self-assembly, electrospinning, and solvent-free hot-pressing	There is a possibility to enhance the membrane mechanical strength, totally control the surface physiochemical properties such as hydrophilicity, charge, and roughness, and to increase the rejection ability in the NF and MD processes	(Li et al.2018, Zirehpour et al. 2017)

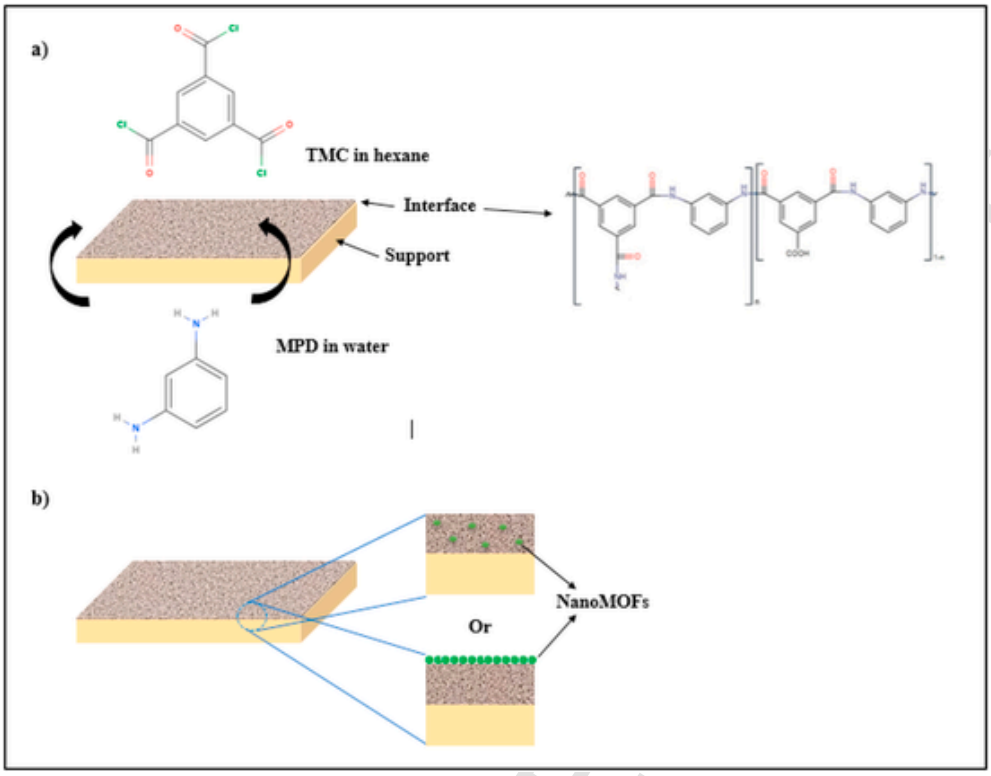

Fig. 8. Schematic view of the (a) TFC membrane made from the IP reaction between TMC and MPD monomers on the substrate and (b) TFN membranes made through incorporation of the nanoMOFs into the TFC membrane.

ganic solution before the IP process. Thus, a PA layer containing MOF nanoparticles was formed on the membrane which was also confirmed by the top-surface and cross-section field emission scanning electron microscopy (FESEM) imaging. It was predicted that, due to the presence of organic linker in the framework of the MOF nanocrystals which can provide hydrogen bonding between 3HBTC and PC, there should be a good compatibility between the MOF nanoparticles and PA layer. According to the FESEM images, the MOF nanoparticles were totally surrounded by the PA layer, which supports their prediction. With the highest amount of MOF nanoparticles in the organic solution (0.08 wt.%), the AL cross-linking degree compared with the control TFC membrane was reduced from 97 to 88 %. The membrane surface hydrophilicity was also increased by increasing the amount of MOF nanoparticles, which can be attributed to the MOF's organic building block containing carboxylic acid groups. The TFN membrane fabricated with 0.04 wt.% MOF nanoparticles showed the best results by considering both the water permeability and salt rejection, in which the water permeability was increased by 129 % in comparison with the control membrane. Also, the FO water flux was increased by 27 % for this membrane which can be definitely assigned to both the higher water permeability and hydrophilicity. This membrane was used for the Caspian seawater desalination and exhibited a boosted and stable performance as compared with the control membrane.

Afterwards, Ma and co-workers incorporated ~~the~~ super-hydrophilic UiO-66 nanoparticles into the PA layer to fabricate a TFN membrane with simultaneously enhanced water flux and selectivity (Ma et al., 2017 a). The main idea of this study was that, due to the molecular-sieving and super hydrophilic nature of the UiO-66 nanoparticles, the morphology and chemistry of the membrane will be significantly altered, leading to improved intrinsic separation properties. They used the same method to form a PA layer containing MOF nanoparticles (0.05, 0.1, 0.15, 0.2 wt.%) onto the polysulfide (PSU) SL to fabricate the target TFN membranes. By increasing the loading percentage of the super-hydrophilic UiO-66 nanoparticles, the membrane hydrophilicity was improved. Because the IP reaction strongly depends on the diffusion of MPD monomers (hydrophilic) from the aqueous solution to the organic solution to react with TMC, this diffusion was facilitated due to the presence of super-hydrophilic UiO-66 nanoparticles, hence, the PA thickness was increased by increasing the loading percentage of nanoparticles. For example, the thickness of the TFN membrane, containing 0.2 wt.% nanoparticles, was about 5 times higher than that of the control TFC membrane. The membrane fouling resistance and water permeability were increased using the modified hydrophilic TFN membrane, but in the case of water permeability, this value was decreased by further enhancement from 0.1 to 2 wt.% due to thicker PA layer. The membrane's salt rejection was maintained at the high level, especially with the highest amounts of UiO-66 nanoparticles, which can be assigned to the thicker PA layer and sub-nanometer pores of these particles rejecting the pass of Na^+ and Cl^- ions. In the FO process, the water flux of the modified membranes was improved with increasing the concentration of NaCl solution as the draw solution (DS) following a linear behavior, indicating an improvement of the negative effect of internal concentration polarization (ICP).

The effects of incorporating nanoMOFs into the PA layer have a broad range including roughness, hydrophilicity, morphological structure, cross-linking degree, and thickness of the membrane surface. The way that these parameters change, has a powerful relationship with the properties of the nanoMOFs being used, such as their particle size, pore volume, aperture size, water-stability, hydrophilicity, functionality, and solidity (Seyedpour et al.,2020 a,b,c). In addition, the method used for incorporating these nanoparticles is also of great importance (Seyedpour et al.,2020b). With in-depth considerations with respect to these characteristics, Xiao and co-workers fabricated UiO-66 and UiO-66-NH_2 modified TFN membranes to evaluate how different incorporation procedures can affect the final membrane properties (Chen et al., 2016). In this study, TMC and piperazine (PIP) monomers were used for IP reaction, and MOF nanoparticles were incorporated in two separate ways: 1) dispersing the nanoparticles in an aqueous solution (PIP/wa-

ter), 2) dispersing the nanoparticles in an organic solution (TMC/*n*-hexane). Since the oleophobic nanoparticles display more uniform dispersions in organic solutions as compared with their agglomeration in aqueous solutions (Mozafari et al.,2019), the TFN membranes fabricated using the organic phase containing MOF nanoparticles feature surfaces with more spherical protrusion morphology and consequently rougher structure. Another reason for this phenomenon is the reaction between MOF nanoparticles and TMC monomers (especially in the case of UiO-66-NH_2), leading to nanoparticles with bigger size. It is worth mentioning that the amino-functionalized MOF (UiO-66-NH_2) nanoparticles exhibit a better water-dispersion and less agglomeration due to their amine functionality. Moreover, adding MOF nanoparticles into the organic phase increases the viscosity of this solution and consequently, the diffusion rate of PIP from aqueous solution to organic solution is reduced, leading to less cross-linked and thinner PA layer with more pore size, which can provide an increased water permeability in nanofiltration (NF) processes. On the other hand, in the case of adding nanoparticles into the aqueous phase, the hydration of Zr-MOF nanoparticles releases heat and enhances the miscibility of the aqueous and organic phases, accelerating the diffusion of PIP to the organic phase in the process of forming the TFN membrane, resulting in a higher thickness and more cross-linked PA layer. The chemical nature of nanomaterials, being used in TFN membranes, can introduce some special properties such as antibacterial and antifouling to the membrane, providing substantial advantages (Wang et al., 2021; Wen et al., 2019). For example, copper is one of the most famous metals with antibacterial properties which has been used in a broad range of applications. Hence, copper-based nanoMOFs can have this attractive property along with their other significant properties (Ling et al.,2015; Li et al., 2019b). Accordingly, Wen and co-workers fabricated anti-biofouling TFN membranes using copper-based water-stable nanoMOFs, CuBTTri (Wen et al.2019; Dechnik et al.,2017). This MOF was synthesized through a reaction between 1,3,5-tris(1H-1,2,3-triazol-5yl) benzene (H_3BTTri) and $CuCl_2.H_2O$. The TFN membranes were fabricated using a conventional IP process between MPD aqueous solution and TMC/MOF organic solution (MOF dosages of 0.05, 0.1, and 0.2 wt.%) on top of the PES SLs. *Pseudomonas aeruginosa* (*P. aeruginosa*) bacteria were used as a model strain to evaluate the antibacterial and anti-biofouling behavior of the membranes in this study. In the IP process, due to the lower concentration of MPD monomers on the top surface of nanoMOFs resulted from the more diffusion path and more resistance of the formed membranes, the cross-linking degree of MPD and TMC was decreased, leading to a higher density of carboxylic acid groups on the surface and consequently lower water contact-angle and higher negative zeta potential. The common ridge-and-valley structure of the PA layer was not changed by incorporating nanoMOFs and the surface roughness of the TFN membranes was also in a same range as the control TFC membrane. Regarding the compatibility between MOF nanoparticles and PA layer, because of the hydrogen bonds and/or possible covalent bonds between nanoMOFs and PA, the MOF nanoparticles were immobilized on the surface more robustly, leading to long-term stability of the TFN membranes. Although the thickness of the PA layer was increased upon increasing the dosage of nanoMOFs, the water permeability was increased from 0.86 to 3.38 L/(m^2.h.bar) which can be attributed to the higher porosity of the MOF nanoparticles, leading to enhanced fractional free-volume due to the disrupted polymer chain packing in the IP process by the presence of MOF nanoparticles and the decreased cross-linking degree of the TFN membranes. Based on the mentioned facts, the membrane rejection ability was improved overall, although the nanoMOFs compensated this negative effect to some extent, especially at the dosage of 0.1 wt.%. Regarding the antibacterial and anti-biofouling performances, the colony forming units (CFU) of the TFN membrane with 1 wt.% nanoMOF was only 3.4 % of the TFC membrane and the water flux decline of this membrane was about two times better than the control membrane. More recently, Bonnet and co-workers synthesized native and functionalized PCN-222 nanorods to fabricate the TFN membranes (Alexis et al., 2008). The solvothermal method alongside with the coordination modulation approach (to control the crystal growth) were used in which the reaction occurred between the meso-tetrakis(4-carboxyphenyl) porphyrin (TCPP) and $ZrOCl_2.8H_2O$. To functionalize the MOF nanorods, their node was modified through binding with hydrophobic myristic acid (MA) (PCN-222-MA), which altered the dimensions of the channel and pore size distribution. The final PCN-222 products were uniform rice-like nanorods of 301 nm in length and 96 nm in diameter. Regarding their internal structure, one-dimensional 37 Å channels along the c-axis flanked by 13 Å micropores were obtained that both water molecules, Na^+ (7.16 Å) and Cl^- (6.64 Å) ions can pass through. The PA thickness was not changed significantly by adding the MOF nanorods. The RO water permeability was increased owing to the formation of new pathways in the PA layer due to the presence of PCN-222 nanorods. Although the salt ions were smaller than the PCN-222 pore size, the membrane rejection was not decreased significantly; a reasonable explanation is that the MPD aqueous solution penetrated into the pore volume during the IP process and formed a layer of PA, leading to partial pore blockage and reduced MOF pore size. According to the FESEM and TEM images, by increasing the MA loading, the MOF agglomeration was increased on the membrane surface which can be due to the more hydrophobic nature of PCN-222-MA nanorods, but in most cases, the MOF agglomerates were completely covered by the PA layer. Based on BET analysis, the accessible pore volume was decreased by adding and increasing the loading percentage of MA into the MOF. Therefore, with a MOF with reduced pore volume and a membrane with approximately unchanged PA layer, the membrane water flux was improved without reducing the membrane rejection (Wilson et al.,2018; Zheng et al., 2017; Zornoza et al., 2013).

4.2. Mixed-matrix membrane (MMM)

The mixed-matrix membrane (MMM) is a composite membrane which is fabricated through the combination of an inorganic or organic/inorganic hybrid material in the form of micro- or nanoparticles (i.e. the dispersed phase, also known as filler) and a polymer matrix (i.e. the continuous phase), as shown in (Fig. 9) (Mao et al., 2019). The MOF-based MMM is a membrane in which the MOF particles are used as the fillers. Not only the MOF-based MMMs are easier and cheaper to scale-up, but also are more stable. One of the main and most common methods for the preparation of MMMs is the blending method, which can be divided into the substrate-based blending and substrate-free blending methods (Mao et al., 2019). Because of the good compatibility between the MOF particles and polymer chain, uniform membranes can be achieved through this approach (Sun et al., 2014).

The substrate-based blending method is generally composed of three steps: (1) Mixing the MOF and polymer in an organic solvent to provide the composite membrane solution; (2) Casting the mixed solution onto a porous substrate using flat membrane casting, dip-coating or spin-coating; and (3) Solvent removal during the solidification or desic-

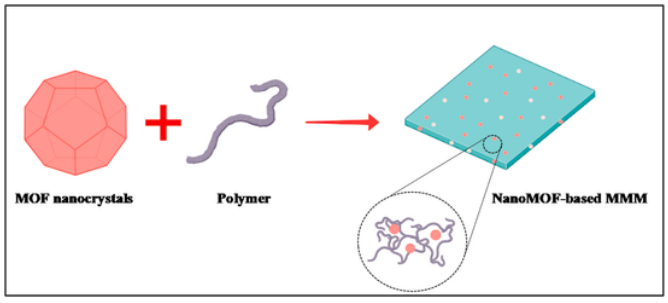

Fig. 9. Schematic representation of nanoMOF-based MMM composed of MOF nanocrystals surrounded by polymer chains.

cation process. For example, Liu et al.2017 mixed ZIF-8 nanoparticles and polymethylphenylsiloxane (PMPS) and then casted the mixed solution onto alumina capillary tubes. This MMM showed an increased permeability towards isobutanol compared with previous reported values. In another work, Li and co-workers prepared a composite membrane by combining super-hydrophobic alkyl-functionalized nanoMOF (RHO-($Zn(eim)_2$)) (MAF-6) and polydimethylsiloxane (PDMS) and then casted the final solution onto poly(vinylidene fluoride) (PVDF) (Hung et al.2014). In comparison with the substrate-based blending technique, the substrate-free blending method is more flexible and easier to delaminate nonporous support from the substrate due to the absence of support. Moreover, the thickness of the final membranes is more controllable simultaneously providing adequate membrane mechanical strength and suitable permeability (51). For example, Arjmandi and co-workers incorporated hydrophilic and hydrophobic nanoMOFs, singular and coupled, into the PES matrix to fabricate MMMs being used as the SLs for TFC-FO membranes in water treatment (Arjmandi et al., 2019; Sethupathy et al., 2013). The ZIF-8 and UiO-66 nanoparticles were synthesized and used as the representatives of hydrophobic and hydrophilic nanoMOFs, respectively.

To ensure the water-stability of these nanoparticles, they were firstly immersed in DI water for 30 h and then used for characterization and fabrication of MMMs. The ZIF-8 nanoparticles showed an octagonal structure with and average diameter of 250 nm and the UiO-66 nanoparticles exhibited spherical morphology with an average diameter of 95 nm. To fabricate the MMMs, the nanoparticles and polymer granules were dissolved in an appropriated solvent and the final solution was casted on a glass plate using a stainless-steel casting knife. The solution containing plate was then immersed in a water bath and maintained for 24 h for a complete PI process. The water contact angle of the fabricated MMMs was increased and decreased in comparison with the neat PES SL, owing to the hydrophobic and hydrophilic nature of the ZIF-8 and UiO-66 nanoparticles, respectively. Interestingly, the water contact angle was not altered in the MMM fabricated with the combination of both nanoparticles due to their opposite wetting properties which neutralized each other. The membrane thickness was not changed; however, the membrane porosity and mean pore size were improved using the MMM approach in all cases which all are great advantages for a SL in the TFC-FO membrane. Under a RO experiment, the pure water permeability was enhanced using the fabricated MMMs instead of the neat PES membrane. In addition, Lin et al. proposed a nanovoid-generated approach based on the blending method by loading HKUST-1 nanoparticles into the PES matrix for the preparation of MMMs (165). To provide a more uniform dispersion of the nanoparticles into the polymer matrix, poly (methyl methacrylate-co-methacrylic acid) (PMMA-co-MAA) copolymer was introduced to the membrane solution to construct a bridge connection between the inorganic nanofillers and the organic matrix. Different loadings of nanofillers and different solidification times in the PI process were considered as the variables in this study. It was found that by increasing the solidification time from 2 to 60 min, the HKUST-1 nanoparticles were diminished gradually which can be attributed to the high hydrophilicity of these particles, leading to their dissolution in the liquid water phase. Accordingly, the MMM surface porosity and pore size were increased upon increasing the solidification period compared with the pristine PES membrane. By increasing the HKUST-1 loading from 0.1 to 0.6 wt.% for 60 min solidification time, the membrane surface pore size (overall porosity) was increased from 10 nm (73.4 %) for the pristine membrane to 42 nm (87.8 %) for the MMM containing 0.6 wt.% of nanoparticles, providing remarkable microstructures available for water permeation. Also, the membrane thickness was not altered considerably, even though, the number and size of nanovoids were increased from the surface to the interior structure. These significant changes in the membrane structure was mainly due to the hydrophilic nature of the nanoparticles, which can reduce the solvent/non-solvent exchange rate, leading to a highly porous structure. It has been claimed that the HKUST-1@mPESMMM featured a high pure water permeability of 490 $L.m^{-2}.h^{-1}.bar^{-1}$, nearly 3 times higher than that of the PES membrane without HKUST-1 nanofillers. A bovine serum albumin (BSA) rejection rate of 96% was maintained without obvious deterioration, showing a significant antifouling effect of this modification strategy.

4.3. Other methods

Except for the two most repeatedly used nanoMOF-based membranes mentioned in the previous subsections, there are some others with more limited reports including porous matrix membranes (PMM) and membranes fabricated by the solvothermal, electrodeposition, vacuum filtration, and surface growth methods. Some of the successful reports regarding these nanoMOF-based membranes are discussed here. The surface growth is a general term for a group of methods in which the nanoMOF is directly synthesized on the membrane surface as a coating instead of the subsequent coating of the already synthesized nanoMOF (Wang et al., 2017; Zhou and Wu, 2015). Therefore, the reaction between metal ion and organic linker occurs in the presence of the membrane and the MOF nanocrystals grow on the membrane surface. Up to now, formation of a MOF film on the membrane was mostly done using the IP and counter-diffusion methods (Efome et al., 2018;Ma et al., 2019). However, due to the presence of two different incompatible solvents and fast intermixing of the precursors in the IP and counter-diffusion processes, respectively, their applications are limited. Zhang and co-workers presented a novel *in situ* method for synthesizing a continuous phase of HKUST-1 nanoMOFs on top of the membrane surface through an electrochemically-assisted interfacial growth (Fig. 10a) (Zhang et al.,2019b). Briefly explaining the used strategy, an electrodeposition process was performed using a copper plate as the cathode and a PES-covered copper plate as the anode in a solution composed of water, 1,3,5-benzenetricarboxylic acid (H_3BTC), and methyltributylammonium methyl sulfate (MTBS). Upon the anodic dissolution of the metal plate, the metal ions were supplied continuously in a controlled manner through applying different current densities. As the metal ions pass through the membrane and make a contact with the linkers in the electrolyte, MOF nanocrystals form on the membrane facing the linkers-containing solution. This laminated membrane was used in the NF process for dye removal from water and exhibited a significant dye rejection ability with an acceptable water flux, as compared with the neat PES membrane. In a novel, simple, one-step method, a layer of MOF nanocrystals was formed on the PES SL using a modified conventional PI process (Figure 10b) (Li et al., 2018). In this method, named as "phase transformation interfacial growth (PTIG)", zinc acetylacetonate ($Zn(acac)_2$) as the precursor for the formation of the ZIF-8 was dissolved in the PES casting solution and the coagulation bath used for the PI process was an aqueous solution of 2-methylimidazole (2-MeIM). Moreover, poly (sodium 4-styrenesulfonate) (PSS) was also added to the casting solution for a hydrophilic modification of the final membrane. During the PTIG process, the PES SL and the continuous ZIF-8 top layer were formed at the same time. It was observed that an ultrathin layer of about 1 μm was formed on the PES SL with no cracks between the two layers, indicating their good mixing and compatibility. In addition, due to the *in-situ* growth of the ZIF-8 layer on the membrane surface and partially into the pores, the PI process was delayed and the complete contraction of the coagulating polymer was interrupted, leading to thicker PES SL. In a dye removal test, the rejection of Congo red was remarkably increased compared with the neat PES membrane and despite the flux reduction, acceptable values were achieved for the water flux. The concentrations of Zn $(acac)_2$ and PSS, and the duration of phase transformation were the dominant factors in this method. The pressure-assisted self-assembly (PASA) technique was vastly investigated in order to form flexible and packed layer of fillers on top of substrates (Ang et al., 2019). Ying and co-workers fabricated

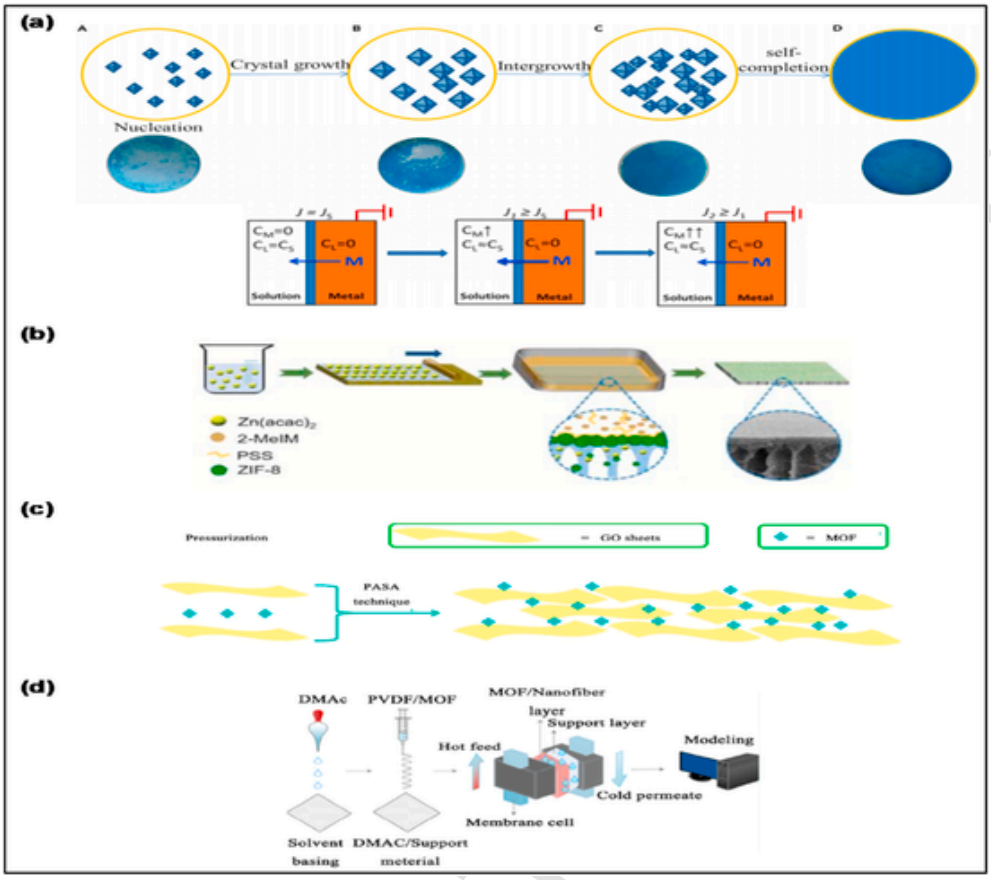

Fig.10. Schematic illustrations of the synthesis of nanoMOF-based composite membranes: (a) electrochemically-assisted interfacial growth (EIG) of the nanoMOFs on the substrate, (b) phase transformation interfacial growth (PTIG) of the nanoMOFs on the substrate, (c) nanoMOF composite membrane by pressure-assisted self-assembly (PASA) technique, (d) electrospinning method. Panel (a) reproduced from reference (Zhang et al.2019)]with permission from the Elsevier Inc., copyright 2019. Panel (b) reproduced from reference (Li et al., 2018) with permission from the Royal Society of Chemistry, copyright 2018. Panel (c) reproduced from reference (Ying et al.,2017) with permission from American Chemical

MOF@~~aphenoG;~~ oxide (GO) membrane based on polyacrylonitrile (PAN) substrate using the PASA technique, as shown in Figure 10c (Ying et al.,2017). The results revealed that the permeate flux for ethyl-acetate/water mixtures was significantly enhanced. MOF nanoparticles can also be added to other layered membrane to produce composite membranes with better separation performance. Electrospinning is a relatively new technology for the preparation of membranes composed of micron and submicron diameter microfibers (Cath et al., 2006; Xu et al., 2010). Due to its various advantages such as low-cost, scalability, and continuous nanofabrication, this technology has widespread applications (Jawad et al., 2020). For example, and co-workers added iron 1,3,5-benzenetricarboxylate MOF (5 wt.% loading) on top of a PVDF substrate through electrospinning method to achieve a superhydrophobic membrane (Figure 10d) (Yang et al.,2018). Due to the presence of MOF, the fiber diameter, pore size, and porosity of the membrane were increased. Much more, Efome and co-workers (Efome et al., 2018; Jawad et al., 2020) produced a composite nanofibrous membrane by electrospinning MOF nanoparticles (Zn-based nanoMOFs) onto polyaniline (PAN) substrate (Gray et al., 2006). In addition to the above-mentioned strategies for combining polymer and MOF nanoparticles for the preparation of nanoMOF-based composite membranes, a novel solvent-free hot-pressing (HoP) method was proposed by Chen et al. 2019a. In this method, the MOF layer is firstly formed on the substrate surface and then uniformly applied on the surface using the HoP process. The solvent-free HoP method was proved to strengthen the MOF layer. Moreover, according to this method, the roll-to-roll process was developed which can more efficiently realize mass production of the MOF coating and lay the foundation for practical production applications (Lin et al.,2019a). The roll-to-roll process allows to control the MOF loading percentage and the particle size.

5. NanoMOF-based membranes applied for water treatment

Membrane-based separation technology is one of the fascinating technologies to eliminate POPs from wastewater due to its high efficiency, easiness to upscale, and the fact that it does not change the phase of the material (Firouzjaei et al.,2020; Zhang et al., 2019c). MOFs-based membranes received a lot of attention from researchers due to their high permeability, selectivity, and photocatalytic activity (Firouzjaei et al.,2020; Zhang et al., 2019c). Generally, MOFs as single building materials of membranes are not applicable since MOFs are expensive and their high crystallinity can produce brittleness, which limits their application in membrane technology (Sun et al., 2019). Thus, MOF-based membranes were commonly grown on support materials i.e., polymers or inorganic materials to reduce cost production and improve their mechanical properties (Jeong et al., 2007, Lee et al., 2011). The other strategy that is massively explored by researchers is mixing polymeric membranes with MOFs as fillers to produce hybrid membranes or mixed matrix membranes (MMM). This strategy is attractive since it offers easy preparation, controllable pores, and is reliable for mass production. In this section, we focus on these two strategies to improve MOFs-based membrane performance for water purification.

5. 1. Growing Metal-Organic Frameworks Crystals on Support Materials

There are several methods that have been developed to prepare pure MOF membranes on support materials, such as *in situ* growth, seed-assisted or secondary growth, and the electrochemical deposition growth methods. In the *in-situ* growth method, MOF crystals were grown on the support surface such as gold (Saleem and Zaidi.,2020), alumina (Lin et al.2019a.b), titanium (Yan et al., 2021), and organic polymers (Eykens et al., 2017). This method is capable of growing MOF crystals with a thickness of 0.3–100 nm. However, inhomogeneous crystal growth on the support surface is often observed, which limits the wide application of this method. Recently, it has been reported that UiO-66-NH_2 MOF deposition on polyacrylonitrile (PAN) substrates through the *in-situ* growth method produces high water permeability of 62 L/m^2.h (LMH) and dye (Rhodamine B) rejection up to 92% (Li et al., 2020b). With the same method, Guo and coworkers reported that UiO-66 on a -wood membrane showed high capability to remove organic pollutants with an efficiency up to 92% and a permeability of 1000 LMH (Dai et al., 2020). Similarly, the formation of MOF membrane on a support can be carried out by seed-assisted or secondary growth. In this method, MOF membrane growth from pre-attached crystal seeds could control nucleation and crystallinity (Li et al., 2020b). MOF membrane prepared by secondary growth method has good performance in gas separation (Mohammad et al., 2015; Shu et al., 2020) and pervaporation (Dai et al., 2020; He et al., 2021). Xu et al. successfully grew Lac-Zn on the polytetrafluoroethylene (PTFE) surface and the resulting membrane exhibited good efficiency for iodide removal (Xu et al.,2010; Samari et al., 2020).

The membranes featured high removal efficiency (92.9%) at a solution pH 6 or 7, but lower for higher and lower pH. On the other hand, the modified Lac-Zn membrane demonstrated high rigidity due to low elasticity and mechanical properties. In another work, MOF-5 was prepared on the alfa-alumina surface (Lovey et al., 2020). The MOF-5 membrane was effective in separation of pure and mixtures of toluene, o-xylene, and 1,3,5-triisopropylbenzene (TIPB). The MOF-5 membrane was prepared in a two-step process, consisting of seed preparation using zinc nitrate hexahydrate and terephthalic acid precursors in dimethylformamide. This was followed by dip-coating and secondary growth by reaction of zinc nitrate hexahydrate, terephthalic acid and *N*-ethyl diisopropylamine in the same medium. Finally, the MOF-5 membrane was activated at 100 °C for 6 h. The produced membrane exhibited higher pervaporation flux for pure component and separation factor for binary mixtures up to 27.7 for toluene/TIPB. The electrochemical deposition (EDS) method was proposed in many works to overcome inhomogeneity of MOF formation by *in situ* and secondary growth methods (Jacob et al.,2020). The MOF membrane was generated *via* the EDS method through anodic dissolution and reductive deprotonation (Rahimi et al.,2021). This method allows the control of the thickness and repairs the MOFs crystal defects. Other advantages of EDS method are low temperature processing, scalability, and short reaction time (Vatanpour et al.,2021). Li et al. 2020 reported ZIF-8 membrane electrochemically deposited onto polyether sulfone (PES) ultrafiltration membrane with various ageing and EDS times. The performance of the produced membrane was characterized by water permeability and salt rejection. ZIF-8 modification resulted in increased surface roughness up to 22.1 ±0.8 nm for 2 min of ageing and EDS times, compared to unmodified membrane roughness that was 2.7 ± 0.1 nm. Water permeability decreased upon increasing the ageing and EDS times, but salt rejection significantly increased. At 2 min ageing and EDS times, high percentages of salt rejection of 90.3% and 96.9% for $MgSO_4$ and Na_2SO_4, respectively, were recorded (Mahdavi et al.,2021).

5. 2. Utilization of Metal-Organic Frameworks as Fillers in Mixed Matrix Membrane (MMM)

Metal-Organic Frameworks as Antifouling Filler: Currently, hydrophobic polymeric-based membranes are the dominant ones in water purification. Polymer materials such as polyethersulfone (PES) (Dehghankar et al.,2021; Zheng et al.,2021a,b), polysulfone (PSU) (Liu et al., 2019a,b), and polyvinylidene fluoride (PVDF) (Wang et al., 2019) are widely used due to their high mechanical properties and chemical resistance. However, the occurrence of fouling on the membrane surface is troublesome that can reduce membrane performance. To overcome this problem, addition of hydrophilic inorganic materials such as clays (Zhou et al., 2020), mesoporous silica (Zhao et al., 2019b), zeolite (Chen et al., 2020) and MOFs (Yang et al., 2017) to form a hybrid membrane or MMM is appealing since it will provide good antifouling properties. MOFs are an attractive class of materials for this purpose due to their tunable surface charge and ability to alter hydrophilicity of membrane matrix. Dehghankar et al. investigated the effect of nanofiller addition (UiO-66, MIL-101 and FAU zeolite) to PVDF membrane on its surface properties, porosity, water permeability, membrane selectivity and anti-fouling properties (Ma et al., 2017b). The addition of inorganic nanofiller improved membrane porosity due to fast liquid-liquid demixing and has larger cavities than pristine PVDF membrane, as confirmed from cross-section FESEM imaging. The produced MMMs exhibited higher surface hydrophilicity and pure water permeability. Membrane selectivity was evaluated for a Bovine Serum Albumin (BSA) solution and achieved rejection rates up to 98%, 100%, and 97% for PVDF/UiO-66 (0.05%); PVDF/MIL-101 (0.1%) and PVDF/FAU (0.1%), respectively. Li and co-workers claimed that HKUST-1 nanofiller modified PES membrane (Makhetha and Moutloali, 2018) generates nanovoids in the membrane surface and increases surface porosity with increasing the nanofiller content. Introduction of poly (methyl methacrylate-co-methacrylic acid) (PMMA-co-MAA) copolymer also increased homogeneity of membrane pores and nanofiller dispersion. PMMA-co-MAA facilitated polar/nonpolar interaction between HKUST-1 and PES polymer chains. The separation performance yielded improvement of pure water fluxes up to 490 LMH and BSA rejection of 96% for PES/HKUS-1 (0.3 wt%). Several researchers showed that MOFs-based MMM technology has high performance in dye filtration (Zheng et al., 2021). Mahdavi et al. loaded MIL-53(Al) onto PSU *via* NIPS to produce PSU-MIL-53 (Al) composite membrane (Li et al., 2020 b). The membrane was characterized for various dyes such as reactive red (RR), direct yellow (DY), methyl green (MG), and crystal violet (CV) rejection. Results showed that the PSU-MIL-53(Al) membrane improved water wettability, permeability (flux), as well as dye rejection. The highest separation performance was recorded for membranes containing 0.06 wt.% MIL-53(Al) with dye rejections of 99.8, 99.5, 99.2, 98.8 and 97.1% for RR, MG, DY, CV, and MB, respectively; pure water flux reached 4.8 LMH. Yang et al. prepared a hybrid membrane using ZIF-8 and polyethyleneimine (PEI) on hydrolyzed polyacrylonitrile (HPAN) substrate (Fig. 11) (Yang et al., 2017). It was found that the addition of ZIF-8/PEI to the HPAN substrate produces defect-free membrane surface with a layer thickness of 556 nm. Increasing the PEI concentration and reaction time resulted in

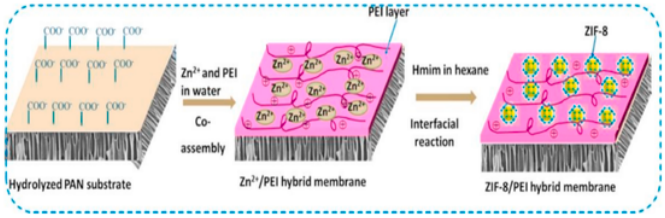

Fig. 11. Schematic illustration of ZIF-8/PEI hybrid membrane preparation process, Reproduced with permission from ref (Yang et al.,2017) Copyright (2017) Elsevier.

lower water permeability, and improved methylene blue (MB) rejection. Long term filtration stability evidently proved that the hybrid ZIF-8/PEI membrane was stable up to three filtration cycles for humic acid (HA) with a flux recovery ratio (FRR)of about 87.7%, Table 4.

In some cases, the addition of the third component into the hybrid membrane constructed by two components turned to be effective in improving the membrane performance, as proposed by Ma et al. 2019. Hybrid MOF/polymer membranes and third component such as graphene oxide (GO) have been reported by several researchers to produce high permeability and selectivity (Hu et al., 2021; Zhang et al., 2021). Makheta et al. described Cu(tpa) MOFs supported on GO and c-ombined with PES to produce Cu(tpa)@GO/PES composite membrane (Heu et al., 2020). The combination of GO and Cu(tpa) in PES membranes influenced the surface roughness and hydrophilicity. The Cu(tpa)@GO/PES composite membrane displayed smoother surface, resulting in lower interaction between contaminant and membrane surface. The membrane hydrophilicity was significantly improved and affected positively water permeability. Lower tortuosity of the composite membrane, confirmed from the cross-section microscopic analysis, facilitated fast water permeation and also supported the water permeability data. Membrane selectivity against CR was achieved, which was evidently confirmed by high rejection rate (more than 80%). Anti-fouling properties of Cu (tpa)@GO/PES composite membrane toward BSA filtration were improved attaining FRR > 80%. In addition, UiO-66@GO/PES composite membrane was successfully produced by Ma et al.2017 *via* phase inversion using various concentrations of UiO-66@GO composite. As a result, the UiO-66@GO/PES membrane has a smoother surface compared to PES pristine membrane (Yang et al., 2019b). The surface hydrophilicity and water flux as well as antifouling properties were improved by increasing UiO-66@GO content. Dye filtration performance for Methyl Orange (MO) and Direct Red (DR) 80 was enhanced with increasing the filler content and the best rejection ratios of DR 80 and MO were 98.3% and 89.0%, respectively, for 3 wt.%. The presence of UiO-66 could hinder stacking of GO in the polymer matrix, resulting in higher membrane selectivity. MOFs as photocatalytic fillers for photocatalytic membrane fouling is initiated by particle deposition on the membrane surface. Membrane modification by altering the surface hydrophilicity is capable to overcome the fouling issue. However, the foulant removal on the membrane surface needs to be achieved through backwash. One effective method to remove foulant without backwash is by introducing a photodegradation feature. In this approach, membrane modification with photocatalytic materials, which are further

Table 4
Some of the successful efforts of using the nanoMOF-based composite membranes in different membrane processes.

Membrane System	MOF Type	Membrane Type	Physiochemical properties	Performance	Ref.
FO	Ag-MOF (Silver I & 3HBTC)	TFN; Incorporation through the IP process	(1) Slightly decreased PA cross-linking degree; (2) Increased surface hydrophilicity	(1) Significantly increased water permeance; (2) Increased FO flux	(Zirehpour et al., 2017)
FO	UiO-66	TFN; Incorporation through the IP process	(1); Significantly increased surface hydrophilicity; (2) Increased PA thickness	(1) Increased water permeance; (2) Increased fouling resistance; (3) High salt rejection; (4)	(Ma et al., 2017)
FO	ZIF-8 & UiO-66	MMM; As the SL for the TFC FO membrane	(1) Increased (UiO-66), decreased (ZIF-8), and unchanged (UiO-66 & ZIF-8) hydrophilicity; (2) Improved porosity and pore size	(1) Decreased dilutive ICP (DICP) due to the channelization; (2) Increased FO flux	(Arjmandi et al., 2019)
FO	Ag-MOF (Silver acetate & NH_2-BDC)	TFN; *in situ* anchoring on the PA layer	(1) Increased surface hydrophilicity; (2) Increased surface roughness; (3) Increased surface negative charge	(1) Slightly decreased water permeance and FO flux; (2) Improved separation and reverse salt flux; (3) Significant antifouling performance; (4) Increased membrane durability	(Seyedpour et al., 2019)
FO	Zn@MOF-5	TF-PMM; An integrated membrane with porous SL	(1) Increased porosity; (2) decreased thickness; (3) Decreased tortuosity	(1) Significantly increased FO flux; (2) High salt rejection; (3) Increased FO flux in seawater desalination and orange juice concentration	(Arjmandi et al., 2019)
NF	UiO-66 & UiO-66-NH_2	TFN; Incorporation through the IP process	MOF in organic phase: (1) Decreased PA cross-linking degree and thickness; (2) Increased PA pore size. MOF in aqueous phase: higher thickness and cross-linking degree of the PA	(1) Increased water permeance in all cases, especially in the case of MOF in organic phase; (2) High separation ability	(Xiao et al.,2019)
NF	BUT-203	TFN; Spin-coating on the substrate	(1) Formation of ultra-thin MOF layer on the substrate; (2) Increased mechanical strength	(1) Increased water permeance; (2) High rejection values against anionic dyes	(Shu et al., 2020)
NF	ED-MIL-101(Cr)	TFN; Incorporation through the IP process	Dually charged surface	(1) Increased water flux; (2) Increased separation efficiency towards the negatively and positively charged PhACs	(Dai et al., 2020)
NF	HKUST-1	Polymer/MOF composite membrane; Surface growth	Formation of a continuous MOF layer on the substrate	(1) Significantly increased removal of the rose Bengal dye compared with the uncoated substrate; (2) Decreased water flux	(Zhang et al.,2019c)
MD	ZIF-71	MOF-coated hollow fiber substrate; Surface growth	(1) Increased surface hydrophobicity; (2) Increased surface roughness	(1) Increased water permeability; (2) Ultra-high salt rejection; (3) Increased wetting resistance	(Li et al., 2020)
MD	Iron 1,3,5-benzenetricarboxylate	MOF-coated substrate; Electrospinning	(1) Increased fiber diameter, pore size, and membrane porosity; (2) Increased hydrophobicity	(1) Increased water permeance; (2) Ultra-high salt rejection; (3) Stable performance	(Yang et al.,2018)
UF	Melamine-functionalized UiO-66-NH_2	MMM; Through the PI process	(1) Increased membrane hydrophilicity; (2) Increased membrane porosity; (3) Increased surface roughness	(1) Increased water flux; (2) Increased antifouling performance and FRR; (3) High rejection values towards milk and oil	(Samari et al.,2020)
UF	HKUST-1	MMM; Through the PI process	(1) Increased membrane porosity and surface pore size; (2) Increased number and size of nanovoids	(1) Three times higher water flux; (2) High rejection; (3) Increased antifouling performance	(Lin et al., 2019b)

known as photocatalytic membrane, is needed. As discussed in the previous Section 3.2, several MOFs own good photocatalytic performance. Thus, the addition of MOFs in polymeric membranes to create photocatalytic membranes is attractive to boost membrane performance in water purification (Baneshi et al.,2020; Sun et al., 2018). Zhou et al. reported self-cleaning, antibacterial, and dye selective properties of MIL-125(Ti)/PVDF photo-catalyst membrane prepared by phase inversion using various concentrations of MIL-125(Ti). The result revealed the optimum composition of the composite membrane achieved a water flux of 64.3 L/m^2.h.bar and a rejection of Rhodamine B (RhB) of 99.7%. Photocatalytic and antibacterial properties of the membrane were examined by exposure to natural light irradiation, resulting in a high flux recovery and RhB rejection by the addition of 10% of MIL-125(Ti) prior to light exposure for three cycles. The photocatalyst reaction on the membrane is achieved due to the light induction at a certain energy level irradiating the MIL-125, which causes an electron promotion to yield a hole, hydroxyl radical, and superoxide free radical. Li et al., 2021 synthesized a nanofibrous MOF membrane and measured the photocatalytic activity for methyl orange (MO) and formaldehyde (FA). This research combines polyacrylic acid (PAA), poly (vinyl alcohol) (PVA), phosphotungstic acid (PW12) and UiO-66 producing PAA-PVA/PW12@UiO-66 nanofibrous membrane by electrospinning. The cross-link occurrence of the membrane was varied between 30–120 s. In this research, a surface modification of PAA-PVA nanofibrous membrane was also conducted by growing the PW12@UiO-66 crystal *via* an *in-situ* approach with the reaction time varied from 3–15 min. The result showed the high photocatalytic activity of both PW12@UiO-66 and PAA-PVA/PW12@UiO-66. The presence of FA in the solution accelerates MO degradation to reach 97.35%. The cross-linking reaction time influences the photodegradation of MO, as witnessed by the highest degradation (97.35%) achieved by 60 s of cross-linking time. MOF-based photocatalytic membranes have also been reported in several other applications, such as oil and water separation (Mamah et al., 2020; Heng et al., 2021), phenol removal (Pramono et al., 2019), and organic pollution (Escorial et al., 2020); all these studies generally demonstrated that MOF addition within the membrane can significantly improve the membrane performance. Summary of MOFs based MMM's performance is presented in Table 5.

6. Final remarks and future prospects

Many MOFs have been developed in recent years, and many of them exhibit unique features. There is likely no limit to the varieties of MOF materials that may be created because a new MOF can be created by coupling different cluster-ligand combinations and also by inserting a different functional group on the surface or in the framework of the MOFs. Producing MOF materials at the nanoscale, on the other hand, is no longer a difficulty, and the number of reports on nanoMOF production is uncountable. With these materials, substantial physical or chemical alteration of membrane structure, which was certainly a pipe dream only a few years ago, is now conceivable.

According to a comprehensive review conducted to develop a comprehensive vision on the subject, nanoMOF synthesis and modification procedures, as well as fabrication methodologies for nanoMOF-based membranes, are constantly evolving. As a result, the adjustability of such membranes' physicochemical properties is fast improving to fulfill the requirements for effective water treatment operations. The methods for fabricating nanoMOF-based membranes can vary depending on the targeted application, as detailed in the previous sections. Membranes that can guarantee high water flux while also being selective for specific solutes are created using these methods.

MOF-based membranes (composite or freestanding MOF membranes) were once solely employed in gaseous systems, but this is no longer the case due to increased water-stability of MOF materials. Furthermore, certain production methods employ this common MOF flaw to create high-yield membranes. The ability to produce cutting-edge nanoMOFs while addressing the membrane difficulties ~~that their mechanisms are well known~~ is a fantastic opportunity to push this well-established separation technology even further, improving its efficiency in water treatment systems. Because nanoMOF materials improved the primary membrane difficulties, fouling, bacterial adhesion and growth, concentration or temperature polarization, low water flux, and poor se-

Table 5
Summary of MOFs-based MMM's performance.

MOFs	Matrix	Feeds	PWF (LMH)	Rejection/Removal (%)	FRR (%)	Ref.
MIL – 101 UiO – 66	PVDF	BSA	360 320	100 98	77.7	(Dehghankar et al., 2021)
HKUST-1	mPES	BSA	490	96	-	(Lin et al.,2019b)
HKUST–1@GO	Cellulose acetate	BSA	183.5	91	88.13	(Yang et al., 2019b)
ZIF-8	PSU	BSA	298	98.5	81.1	(Sun et al.,2018)
MIL- 53(Al)	PSU	Reactive Red (RR) Direct Yellow (DY) Methyl Green (MG) Crystal Violet (CV) Methylene Blue (MB)	4.8	99.8 99.2 99.5 98.8 97.1	-	(Mahdavi et al.,2021)
UiO-66	Polyethyleneimine (PEI)/PAN	Congo Red (CR)	14.8	99.9		(Wang et al., 2019; Gómez-Avilés et al., 2019)
ZIF-8	Cellulose	Rhodamine B(RhB)	14.1	96	> 90	(Chen et al., 2020)
ZIF-8	Polyethyleneimine (PEI)/hydrolyzed Polyacrylonitrile (HPAN)	Methylene Blue (MB) Humic Acid (HA) BSA	33	99.6 - -	- 87.8 83.3	(Yang et al., 2017)
MOF-2(Cd)	Polyimide	Methylene Blue (MB) Eosin Y	117.8- 171.4	99.9 81.2	-	(Baneshi et al.,2020)
MIL-125(Ti)	PVDF (Photocatalytic membrane)	Rhodamine B(RhB)	64.3	99.7	~ 100	(Zhou et al.,2020)
PW12@UiO-66	PAA-PVA (Photocatalytic membrane)	Methyl Orange (MO)	-	97.35	-	(Li et al.,2021)
MIL-88B(Fe)	Al_2O_3 hollow (Photocatalytic membrane)	Phenol	4000-4500	95	~ 94%	(Hu et al.,2021)
UiO-66@GO	Polyamide NF (Photocatalytic membrane)	Suw annee River humic acid Carbamazepine (CBZ) Diclofenac sodium (DCF)	63	- 70% 93%	97 -	(Heu et al., 2020)

lectivity were all thoroughly discussed in this review. Significant progress has been achieved in the use of nanoMOFs in membrane processes such as FO, RO, MD, NF, and UF in water treatment since their introduction in environmental applications.

To date, many manufacturing processes have been employed to construct nanoMOF-based membranes, including TFN, MMM, PMM, solvothermal, electrodeposition, vacuum filtering, and surface growth, with the goal of achieving membranes with customized properties. Various nanoMOFs (e.g. UiO-66, ZIF-8, CuBTTri, MOF-5, HKUST, BUT-203, MIL-101(Cr), and ZIF-71) were introduced into the structure or on the surface of conventional thin polymeric films (e.g. PES, PA, PSU, and PVDF) to add valuable functionalities such as high water flux, enhanced selectivity, and robust antifouling properties to the membranes via the following mechanisms: (i) nanoMOF-based membranes contain highly variable porosities, additional channels, and a large accessible surface area, all of which can let water molecules pass through the membrane more easily, and (ii) due to steric exclusion and electrostatic repulsion, these hydrophilic/hydrophobic nanoMOFs have the unique capacity to combine species/special functions without changing the framework topology, which is useful for reducing membrane fouling and boosting selectivity. Furthermore, including nanoMOFs into the membrane structure improves its durability and ensures the production of long-lasting membranes, which are necessary for industrial applications. These nanoMOF-based research, on the other hand, ~~were~~ primarily confined to a few nanoMOF materials and pollutants (mainly NaCl and dyes). As a result, a thorough examination of various nanoMOF-based membranes, pollutants, and water quality is still required.

The following are the most significant issues in this field of study: (i) creating innovative nanoMOF synthetic and post-treatment procedures, as well as increasing the efficacy of incorporation techniques to reduce membrane shortage, (ii) understanding how different types of MOF nanomaterials affect membrane production and critical features like hydrophilicity, pore size, and surface roughness, all of which are influenced by MOF/casting solution interactions, and (iii) a trade-off between water permeability and selectivity of nanoMOF-based membranes in order to analyze transition mechanisms in the presence of various background ions and natural organic matter in order to replicate natural water and examine large-scale membrane stability in long-term processes.

The chemical stability of the nanoMOFs contained in each membrane, as well as the hydrolytic stability of nanoMOF-based membranes, are critical factors to consider when assessing these membranes in water treatment systems. The solution pH during membrane filtration, in particular, may cause degradation of specific MOF structures and possibly damage or complete change of the original phase, resulting in reduced filtration capacity and, in extreme situations, catastrophic collapse.

However, this is merely a management strategy and not a guarantee, as there are a number of other factors that could prevent these processes from taking place. Furthermore, because the current high cost of synthesis of nanoMOFs is a major barrier to large-scale applications of nanoMOF-based membranes, new synthetic methodologies based on low-cost, readily available raw materials are critical. Because the focus of this review is on membrane performance in water treatment applications, a thorough understanding of the systemic transition mechanisms of vital aqueous species in nanoMOF-based membranes in terms of membrane porosity, host-guest interactions, and macroscopic fluid dynamics is still required.

Uncited References

Akbari and Peyravi, 2020, Arjmandi et al., 2019b, Cai et al., 2019c, Cai et al., 2019b, Crini et al., 2018, Ding and Jiang, 2021, Gajanan and Tijare, 2018, Gao et al., 2019b, Li et al., 2019a, Li et al., 2017a, Li et al., 2017b, Lin et al., 2019b, Mamah et al., 2021, Má rquez et al., 2012, Nguyen and Cohen, 2010, Saleem and Zaidi, 2020, Zhang et al., 2020, Zhang et al., 2022, Zhao et al., 2018b, Zhao et al., 2018a, Zheng et al., 2021b

Declaration of competing interest

The authors declare that they have no known competing financial interests or personal relationships that could have appeared to influence the work reported in this paper.

References

Abdi, J., Abedini, H., 2020. MOF-based polymeric nanocomposite beads as an efficient adsorbent for wastewater treatment in batch and continuous systems: Modelling and experiment. Chem. Eng.J. 400, 125862.

Akbari, S., Peyravi, M., 2020. Improving water flux and salt rejection by a tradeoff between hydrophilicity and hydrophobicity of sublayer in TFC FO membrane. Chem. Eng. Res. and Design 162, 94–106.

Alexis, F., Pridgen, E., Molnar, L.K., Farokhzad, O.C., 2008. Factors affecting the clearance and biodistribution of polymeric nanoparticles. Molecular Pharmaceutics 5 (4), 505–515.

Arjmandi, A., Peyravi, M., Arjmandi, M., Altaee, A., 2020a. Exploring the use of cheap natural raw materials to reduce the internal concentration polarization in thin-film composite forward osmosis membranes. Chem. Eng. J. 398, 125483.

Arjmandi, M., Peyravi, M., Chenar, M.P., Jahanshahi, M., 2019a. Channelization of water pathway and encapsulation of DS in the SL of the TFC FO membrane as a novel approach for controlling dilutive internal concentration polarization. Env. Sci.: Water Res. Tech. 5 (8), 1436–1452.

Arjmandi, M., Peyravi, M., Chenar, M.P., Jahanshahi, M., 2019b. A new concept of MOF-based PMM by modification of conventional dense film casting method: Significant impact on the performance of FO process. J. Membrane Sci. 579, 253–265.

Arjmandi, M., Pourafshari Chenar, M., Peyravi, M., Jahanshahi, M., 2020b. Physical modification of polymeric support layer for thin film composite forward osmosis membranes by metal–organic framework-based porous matrix membrane strategy. J. App. Poly. Sci. 137 (19), 48672.

Ayala, S., Bentz, K.C., Cohen, S.M., 2019. Block co-polyMOFs: morphology control of polymer–MOF hybrid materials. Chem. Sci. 10 (6), 1746–1753.

Baneshi, M.M., Ghaedi, A.M., Vafaei, A., Emadzadeh, D., Lau, W.J., Marioryad, H., Jamshidi, A., 2020. A high-flux P84 polyimide mixed matrix membranes incorporated with cadmium-based metal organic frameworks for enhanced simultaneous dyes removal: Response surface methodology. Environmental Research 183, 109278. https://doi.org/10.1016/j.envres.2020.109278.

Batra, R., Chen, C., Evans, T.G., Walton, K.S., Ramprasad, R., 2020. Prediction of water stability of metaorganic frameworks using machine learning. Nature Machine Intelligence 2, 704–710.

Bedia, J., Muelas-Ramos, V., Peñas-Garzón, M., Gómez-Avilés, A., Rodríguez, J.J., Belver, C., 2019. A review on the synthesis and characterization of metal organic frameworks for photocatalytic water purification. Catalysts 9 (1), 52.

Bernal, V., Giraldo, L., Moreno-Piraján, J.C., 2021. Physicochemical Parameters of the Methylparaben Adsorption from Aqueous Solution Onto Activated Carbon and Their Relationship with the Surface Chemistry. ACS Omega 6 (13), 8797–8807.

Bernal, V., Giraldo, L., Moreno-Piraján, J.C., 2018. Acetaminophen adsorption on activated carbons at different pH. Change of enthalpy and entropy of the process. Revista Colombiana de Química 47 (2), 54–62.

Bernal, V., Giraldo, L., Moreno-Piraján, J.C., 2020. A new methodology to determine the effect of the adsorbate-adsorbent interactions on the analgesic adsorption onto activated carbon using kinetic and calorimetry data. Environmental Science and Pollution Research 27 (29), 36639–36650.

Bhushan, B., Bhushan, B., Baumann, 2007. Springer handbook of nanotechnology, 2. Springer.

Boles, M.A., Ling, D., Hyeon, T., Talapin, D.V., 2016. The surface science of nanocrystals. Nature Materials 15 (2), 141–153.

Bonnett, B.L., Smith, E.D., De La Garza, M., Cai, M., Haag IV, J.V., Serrano, J.M., Cornell, H.D., Gibbons, B., Martin, S.M., Morris, A.J., 2020. PCN-222 Metal–Organic Framework Nanoparticles with Tunable Pore Size for Nanocomposite Reverse Osmosis Membranes. ACS App. Mat. Inter. 12 (13), 15765–15773.

Burtch, N.C., Jasuja, H., Walton, K.S., 2014. Water stability and adsorption in metal–organic frameworks. Chemical Reviews 114 (20), 10575–10612.

Cai, W., Wang, J., Chu, C., Chen, W., Wu, C., Liu, G., 2019a. Metal–organic framework-based stimuli-responsive systems for drug delivery. Adv. Sci. 6 (1), 1801526.

Cai, X., Deng, X., Xie, Z., Shi, Y., Pang, M., Lin, J., 2019c. Controllable synthesis of highly monodispersed nanoscale Fe-soc-MOF and the construction of Fe-soc-MOF@ polypyrrole core-shell nanohybrids for cancer therapy. Chem. Eng. J. 358, 369–378.

Cai, X., Lin, J., Pang, M., 2016. Facile synthesis of highly uniform Fe-MIL-88B particles. Cry. Grow. Des. 16 (7), 3565–3568.

Cai, X., Liu, B., Pang, M., Lin, J., 2018. Interfacially synthesized Fe-soc-MOF nanoparticles combined with ICG for photothermal/photodynamic therapy. Dalton Trans 47 (45), 16329–16336.

Cai, X., Xie, Z., Li, D., Kassymova, M., Zang, S.-Q., Jiang, H.-L., 2020. Nano-sized metal-organic frameworks: Synthesis and applications. Coord. Chem. Revi. 417, 213366.

Cai, X., Xie, Z., Pang, M., Lin, J., 2019b. Controllable synthesis of highly uniform nanosized HKUST-1 crystals by liquid–solid–solution method. Crys. Grow. Des. 19

(2), 556–561.
Chalati, T., Horcajada, P., Gref, R., Couvreur, P., Serre, C., 2011. Optimisation of the synthesis of MOF nanoparticles made of flexible porous iron fumarate MIL-88A. J. Mat. Chem. 21 (7), 2220–2227.
Cath, T.Y., Childress, A.E., Elimelech, M., 2006. Forward osmosis: Principles, applications, and recent developments. Journal of Membrane Science 281 (1), 70–87. https://doi.org/10.1016/j.memsci.2006.05.048.
Chen, L., Wang, F., Yang, W., Gu, D., Li, M., Pan, Q., 2020. Cellulose Membrane Composited with ZIF-8 for Selective Separation of Rhodamine B. ChemistrySelect 5 (13), 4078–4084. https://doi.org/10.1002/slct.202000977.
Chen, Y., Li, S., Pei, X., Zhou, J., Feng, X., Zhang, S., Cheng, Y., Li, H., Han, R., Wang, B., 2016. A Solvent-Free Hot-Pressing Method for Preparing Metal–Organic-Framework Coatings. Angewandte Chemie Int. Ed. 55 (10), 3419–3423.
Chen, Y.-Z., Zhang, R., Jiao, L., Jiang, H.-L., 2018. Metal–organic framework-derived porous materials for catalysis. Coord. Chem. Rev. 362, 1–23.
Chen, X., Wang, D., Wang, T., Yang, Z., Zou, X., Wang, P., Luo, W., Li, Q., Liao, L., Hu, W., 2019a. Enhanced photoresponsivity of a GaAs nanowire metal-semiconductor-metal photodetector by adjusting the fermi level. ACS Appl. Mater. Interfaces. 11 (36), 33188–33193.
Chen, C., Feng, X., Zhu, Q., Dong, R., Yang, R., Cheng, Y., He, C., 2019b. Microwave-assisted rapid synthesis of well-shaped MOF-74 (Ni) for CO2 efficient capture. Inorg. Chem. 58 (4), 2717–2728.
Cravillon, J., Munzer, S., Lohmeier, S.-J., Feldhoff, A., Huber, K., Wiebcke, M., 2009. Rapid room-temperature synthesis and characterization of nanocrystals of a prototypical zeolitic imidazolate framework. Chem. Mat. 21 (8), 1410–1412.
Crini, G., Lichtfouse, E., Wilson, L.D., Morin-Crini, N., 2018. Conventional and non-conventional adsorbents for wastewater treatment. Environmental Chemistry Letters 17, 195–213.
Dai, R., Wang, X., Tang, C.Y., Wang, Z., 2020. Dually charged MOF-based thin-film nanocomposite nanofiltration membrane for enhanced removal of charged pharmaceutically active compounds. Environmental Science & Technology 54 (12), 7619–7628.
Dechnik, J., Gascon, J., Doonan, C.J., Janiak, C., Sumby, C.J., 2017. Mixed-matrix membranes. Angewandte Chemie International Edition 56 (32), 9292–9310.
DeCoste, J.B., Peterson, G.W., Jasuja, H., Glover, T.G., Huang, Y., Walton, K.S., 2013. Stability and degradation mechanisms of metal–organic frameworks containing the Zr6O4(OH)4 secondary building unit. J. Mater. Chem. A 1 (18), 5642–5650. https://doi.org/10.1039/C3TA10662D.
Dehghankar, M., Mohammadi, T., Moghadam, M.T., Tofighy, M.A., 2021. Metal-organic framework/zeolite nanocrystal/polyvinylidene fluoride composite ultrafiltration membranes with flux/antifouling advantages. Materials Chemistry and Physics 260, 124128. https://doi.org/10.1016/j.matchemphys.2020.124128.
Deng, Y., Wu, Y., Chen, G., Zheng, X., Dai, M., Peng, C., 2021. Metal-organic framework membranes: Recent development in the synthesis strategies and their application in oil-water separation. Chemical Engineering Journal 405, 127004. https://doi.org/10.1016/j.cej.2020.127004.
de Franco, M.A.E., de Carvalho, C.B., Bonetto, M.M., de Pelegrini Soares, R., Féris, L.A., 2018. Diclofenac removal from water by adsorption using activated carbon in batch mode and fixed-bed column: Isotherms, thermodynamic study and breakthrough curves modeling. Journal of Cleaner Production 181, 145–154. https://doi.org/10.1016/j.jclepro.2018.01.138.
Ding, C., Yin, J., Deng, B., 2014. Effects of polysulfone (PSf) support layer on the performance of thin-film composite (TFC) membranes. Journal of Chemical and Process Engineering 1 (102), 1–8.
Ding, M., Jiang, H.-L., 2021. Improving water stability of metal–organic frameworks by a general surface hydrophobic polymerization. CCS Chemistry 3 (8), 2740–2748.
Diring, S., Furukawa, S., Takashima, Y., Tsuruoka, T., Kitagawa, S., 2010. Controlled Multiscale Synthesis of Porous Coordination Polymer in Nano/Micro Regimes. Chemistry of Materials 22, 4531–4538.
Drache, F., Bon, V., Senkovska, I., Marschelke, C., Synytska, A., Kaskel, S., 2016. Postsynthetic inner-surface functionalization of the highly stable zirconium-based metal–organic framework DUT-67. Inorganic Chemistry 55 (15), 7206–7213.
Efome, J.E., Rana, D., Matsuura, T., Lan, C.Q., 2018. Insight studies on metal-organic framework nanofibrous membrane adsorption and activation for heavy metal ions removal from aqueous solution. ACS Applied Materials & Interfaces 10 (22), 18619–18629.
El Khames Saad, M., Khiari, R., Elaloui, E., Moussaoui, Y., 2014. Adsorption of anthracene using activated carbon and Posidonia oceanica. Arabian Journal of Chemistry 7 (1), 109–113. https://doi.org/10.1016/j.arabjc.2013.11.002.
Escorial, J.G., Lanzanas, S.P., Berjamin, K.J., Caliolio, M.H., Dimaunahan, E., Lagura, V., Milo, L., Basilia, B., 2020. Development and physico-chemical characterization of Polyvinylidene fluoride ({PVDF}) flat sheet membranes with antibacterial properties against E. coli and S. aureus. Journal of Physics: Conference Series 1593, 12042. https://doi.org/10.1088/1742-6596/1593/1/012042.
Eykens, L., De Sitter, K., Dotremont, C., Pinoy, L., Van der Bruggen, B., 2017. Membrane synthesis for membrane distillation: A review. Separation and Purification Technology 182, 36–51. https://doi.org/10.1016/j.seppur.2017.03.035.
Ettlinger, R., Sönksen, M., Graf, M., Moreno, N., Denysenko, D., Volkmer, D., Kerl, K., Bunzen, H., 2018. Metal–organic framework nanoparticles for arsenic trioxide drug delivery. J. Mater. Chem. B 6 (40), 6481–6489. https://doi.org/10.1039/C8TB01899E.
Fazal-ur-Rehman, M., 2018. Novel applications of nanomaterials and nanotechnology in medical sciences-a review. J. Basic Appl. Sci. Res 8 (4), 1.
Feng, D., Gu, Z.-Y., Li, J.-R., Jiang, H.-L., Wei, Z., Zhou, H.-C., 2012. Zirconium-Metalloporphyrin PCN-222: Mesoporous Metal–Organic Frameworks with Ultrahigh Stability as Biomimetic Catalysts. Angewandte Chemie International Edition 51 (41), 10307–10310. https://doi.org/10.1002/anie.201204475.
Feng, M., Zhang, P., Zhou, H.-C., Sharma, V.K., 2018. Water-stable metal-organic frameworks for aqueous removal of heavy metals and radionuclides: A review. Chemosphere 209, 783–800. https://doi.org/10.1016/j.chemosphere.2018.06.114.
Firouzjaei, M.D., Seyedpour, S.F., Aktij, S.A., Giagnorio, M., Bazrafshan, N., Mollahosseini, A., Samadi, F., Ahmadalipour, S., Firouzjaei, F.D., Esfahani, M.R., Tiraferri, A., Elliott, M., Sangermano, M., Abdelrasoul, A., McCutcheon, J.R., Sadrzadeh, M., Esfahani, A.R., Rahimpour, A., 2020. Recent advances in functionalized polymer membranes for biofouling control and mitigation in forward osmosis. Journal of Membrane Science 596, 117604. https://doi.org/10.1016/j.memsci.2019.117604.
Fraceto, L.F., de Lima, R., Oliveira, H.C., Ávila, D.S., Chen, B., 2018. Future trends in nanotechnology aiming environmental applications. Springer.
Gajanan, K., Tijare, S.N., 2018. Applications of nanomaterials. Materials Today: Proceedings 5 (1), 1093–1096.
Ganguli, A.K., Ganguly, A., Vaidya, S., 2010. Microemulsion-based synthesis of nanocrystalline materials. Chemical Society Reviews 39 (2), 474–485.
Gao, Q., Xu, J., Bu, X.-H., 2019a. Recent advances about metal–organic frameworks in the removal of pollutants from wastewater. Coordination Chemistry Reviews 378, 17–31.
Gao, T., Li, C., Jia, D., Zhang, Y., Yang, M., Wang, X., Cao, H., Li, R., Ali, H.M., Xu, X., 2020. Surface morphology assessment of CFRP transverse grinding using CNT nanofluid minimum quantity lubrication. Journal of Cleaner Production 277, 123328.
Gao, T., Li, C., Zhang, Y., Yang, M., Jia, D., Jin, T., Hou, Y., Li, R., 2019b. Dispersing mechanism and tribological performance of vegetable oil-based CNT nanofluids with different surfactants. Tribology International 131, 51–63.
Gascon, J., Corma, A., Kapteijn, F., Llabres i Xamena, F.X., 2014. Metal organic framework catalysis: quo vadis? Acs Catalysis 4 (2), 361–378.
Ghasemzadeh, G., Momenpour, M., Omidi, F., Hosseini, M.R., Ahani, M., Barzegari, A., 2014. Applications of nanomaterials in water treatment and environmental remediation. Frontiers of Environmental Science & Engineering 8 (4), 471–482.
Gómez-Avilés, A., Peñas-Garzón, M., Bedia, J., Dionysiou, D.D., Rodríguez, J.J., Belver, C., 2019. Mixed Ti-Zr metal-organic-frameworks for the photodegradation of acetaminophen under solar irradiation. Applied Catalysis B: Environmental 253, 253–262.
Gray, G.T., McCutcheon, J.R., Elimelech, M., 2006. Internal concentration polarization in forward osmosis: role of membrane orientation. Desalination 197 (1), 1–8. https://doi.org/10.1016/j.desal.2006.02.003.
Gu, Y., Huang, M., Zhang, W., Pearson, M.A., Johnson, J.A., 2019. PolyMOF nanoparticles: dual roles of a multivalent polyMOF ligand in size control and surface functionalization. Angewandte Chemie International Edition 58 (46), 16676–16681.
Han, X., Xu, K., Taratula, O., Farsad, K., 2019. Applications of nanoparticles in biomedical imaging. Nanoscale 11 (3), 799–819.
Haque, E., Jhung, S.H., 2011. Synthesis of isostructural metal–organic frameworks, CPO-27s, with ultrasound, microwave, and conventional heating: Effect of synthesis methods and metal ions. Chemical Engineering Journal 173 (3), 866–872. https://doi.org/10.1016/j.cej.2011.08.037.
Haque, E., Jun, J.W., Jhung, S.H., 2011. Adsorptive removal of methyl orange and methylene blue from aqueous solution with a metal-organic framework material, iron terephthalate (MOF-235). Journal of Hazardous Materials 185 (1), 507–511. https://doi.org/10.1016/j.jhazmat.2010.09.035.
He, T., Xu, X., Ni, B., Wang, H., Long, Y., Hu, W., Wang, X., 2017. Fast and scalable synthesis of uniform zirconium-, hafnium-based metal–organic framework nanocrystals. Nanoscale 9 (48), 19209–19215.
He, X., Zhang, T., Xue, Q., Zhou, Y., Wang, H., Bolan, N.S., Jiang, R., Tsang, D.C.W., 2021. Enhanced adsorption of Cu(II) and Zn(II) from aqueous solution by polyethyleneimine modified straw hydrochar. Science of The Total Environment 778, 146116. https://doi.org/10.1016/j.scitotenv.2021.146116.
Heng, Z.W., Tan, Y.Y., Chong, W.C., Mahmoudi, E., Mohammad, A.W., Teoh, H.C., Sim, L.C., Koo, C.H., 2021. Preparation of a novel polysulfone membrane by incorporated with carbon dots grafted silica from rice husk for dye removal. Journal of Water Process Engineering 40, 101805. https://doi.org/10.1016/j.jwpe.2020.101805.
Hermes, S., Witte, T., Hikov, T., Zacher, D., Bahnmüller, S., Langstein, G., Huber, K., Fischer, R.A., 2007. Trapping metal-organic framework nanocrystals: an in-situ time-resolved light scattering study on the crystal growth of MOF-5 in solution. Journal of the American Chemical Society 129 (17), 5324–5325.
Hester, J.G., Kim, S., Bito, J., Le, T., Kimionis, J., Revier, D., Saintsing, C., Su, W., Tehrani, B., Traille, A., 2015. Additively manufactured nanotechnology and origami-enabled flexible microwave electronics. Proceedings of the IEEE 103 (4), 583–606.
Heu, R., Ateia, M., Yoshimura, C., 2020. Photocatalytic Nanofiltration Membrane Using Zr-MOF/GO Nanocomposite with High-Flux and Anti-Fouling Properties. Catalysts 10 (6). https://doi.org/10.3390/catal10060711.
Hou, L., Wang, L., Zhang, N., Xie, Z., Dong, D., 2016. Polymer brushes on metal–organic frameworks by UV-induced photopolymerization. Polymer Chemistry 7 (37), 5828–5834.
Hu, C., Yoshida, M., Huang, P.-H., Tsunekawa, S., Hou, L.-B., Chen, C.-H., Tung, K.-L., 2021. MIL-88B(Fe)-coated photocatalytic membrane reactor with highly stable flux and phenol removal efficiency. Chemical Engineering Journal 418, 129469. https://doi.org/10.1016/j.cej.2021.129469.
Huang, X., Chen, Y., Feng, X., Hu, X., Zhang, Y., Liu, L., 2020. Incorporation of oleic acid-modified Ag@ ZnO core-shell nanoparticles into thin film composite membranes for enhanced antifouling and antibacterial properties. Journal of Membrane Science 602, 117956.
Hung, W.-S., An, Q.-F., De Guzman, M., Lin, H.-Y., Huang, S.-H., Liu, W.-R., Hu, C.-C., Lee, K.-R., Lai, J.-Y., 2014. Pressure-assisted self-assembly technique for fabricating composite membranes consisting of highly ordered selective laminate layers of amphiphilic graphene oxide. Carbon 68, 670–677.

Ismail, A.F., Khulbe, K.C., Matsuura, T., 2015. Gas separation membranes, 10. Switz. Springer, pp. 973–978.
Jacob, L., Joseph, S., Varghese, L.A., 2020. Polysulfone/MMT mixed matrix membranes for hexavalent chromium removal from wastewater. Arabian Journal for Science and Engineering 45 (9), 7611–7620.
Jawad, J., Hawari, A.H., Zaidi, S., 2020. Modeling of forward osmosis process using artificial neural networks (ANN) to predict the permeate flux. Desalination 484, 114427. https://doi.org/10.1016/j.desal.2020.114427.
Jeong, B.-H., Hoek, E.M.V., Yan, Y., Subramani, A., Huang, X., Hurwitz, G., Ghosh, A.K., Jawor, A., 2007. Interfacial polymerization of thin film nanocomposites: A new concept for reverse osmosis membranes. Journal of Membrane Science 294 (1), 1–7. https://doi.org/10.1016/j.memsci.2007.02.025.
Jun, B.-M., Al-Hamadani, Y.A.J., Son, A., Park, C.M., Jang, M., Jang, A., Kim, N.C., Yoon, Y., 2020. Applications of metal-organic framework based membranes in water purification: A review. Separation and Purification Technology, p. 116947.
Juan-Alcañiz, J., Gielisse, R., Lago, A.B., Ramos-Fernandez, E.V., Serra-Crespo, P., Devic, T., Guillou, N., Serre, C., Kapteijn, F., Gascon, J., 2013. Towards acid MOFs – catalytic performance of sulfonic acid functionalized architectures. Catal. Sci. Technol. 3 (9), 2311–2318. https://doi.org/10.1039/C3CY00272A.
Kadhom, M., Deng, B., 2018. Metal-organic frameworks (MOFs) in water filtration membranes for desalination and other applications. Applied Materials Today 11, 219–230.
Kahn, J.S., Freage, L., Enkin, N., Garcia, M.A.A., Willner, I., 2017. Stimuli-Responsive DNA-Functionalized Metal–Organic Frameworks (MOFs). Advanced Materials 29 (6), 1602782.
Karagiaridi, O., Bury, W., Mondloch, J.E., Hupp, J.T., Farha, O.K., 2014. Solvent-Assisted Linker Exchange: An Alternative to the De Novo Synthesis of Unattainable Metal–Organic Frameworks. Angewandte Chemie International Edition 53 (18), 4530–4540. https://doi.org/10.1002/anie.201306923.
Kårelid, V., Larsson, G., Björlenius, B., 2017. Effects of recirculation in a three-tank pilot-scale system for pharmaceutical removal with powdered activated carbon. Journal of Environmental Management 193, 163–171.
Kitagawa, S., 2014. Metal–organic frameworks (MOFs). Chemical Society Reviews 43 (16), 5415–5418.
Kumar, P., Bansal, V., Kim, K.-H., Kwon, E.E., 2018. Metal-organic frameworks (MOFs) as futuristic options for wastewater treatment. Journal of Industrial and Engineering Chemistry 62, 130–145.
Lai, J., Niu, W., Luque, R., Xu, G., 2015. Solvothermal synthesis of metal nanocrystals and their applications. Nano Today 10 (2), 240–267.
Lau, W.J., Gray, S., Matsuura, T., Emadzadeh, D., Chen, J.P., Ismail, A.F., 2015. A review on polyamide thin film nanocomposite (TFN) membranes: History, applications, challenges and approaches. Water Research 80, 306–324.
Lee, K.P., Arnot, T.C., Mattia, D., 2011. A review of reverse osmosis membrane materials for desalination—Development to date and future potential. Journal of Membrane Science 370 (1), 1–22. https://doi.org/10.1016/j.memsci.2010.12.036.
Lee, J.-Y., She, Q., Huo, F., Tang, C.Y., 2015. Metal–organic framework-based porous matrix membranes for improving mass transfer in forward osmosis membranes. Journal of Membrane Science 492, 392–399.
Lee, S., Sasaki, D., Kim, D., Mori, M., Yokota, T., Lee, H., Park, S., Fukuda, K., Sekino, M., Matsuura, K., 2019. Ultrasoft electronics to monitor dynamically pulsing cardiomyocytes. Nature Nanotechnology 14 (2), 156–160.
Lee, Y.-J., Chang, Y.-J., Lee, D.-J., Hsu, J.-P., 2018. Water stable metal-organic framework as adsorbent from aqueous solution: A mini-review. Journal of the Taiwan Institute of Chemical Engineers 93, 176–183. https://doi.org/10.1016/j.jtice.2018.06.035.
Li, B., Wen, H.-M., Zhou, W., Chen, B., 2014. Porous metal–organic frameworks for gas storage and separation: what, how, and why? The Journal of Physical Chemistry Letters 5 (20), 3468–3479.
Li, H., Li, L., Lin, R.-B., Zhou, W., Zhang, Z., Xiang, S., Chen, B., 2019a. Porous metal-organic frameworks for gas storage and separation: Status and challenges. EnergyChem 1 (1), 100006.
Li, H., Liu, H., Shi, W., Zhang, H., Zhou, R., Qin, X., 2020a. Preparation of hydrophobic zeolitic imidazolate framework-71 (ZIF-71)/PVDF hollow fiber composite membrane for membrane distillation through dilute solution coating. Separation and Purification Technology 251, 117348.
Li, J., Wang, H., Yuan, X., Zhang, J., Chew, J.W., 2020b. Metal-organic framework membranes for wastewater treatment and water regeneration. Coordination Chemistry Reviews 404, 213116.
Li, Q., Cheng, L., Shen, J., Shi, J., Chen, G., Zhao, J., Duan, J., Liu, G., Jin, W., 2017a. Improved ethanol recovery through mixed-matrix membrane with hydrophobic MAF-6 as filler. Separation and Purification Technology 178, 105–112.
Li, Q., Li, J., Fang, X., Liao, Z., Wang, D., Sun, X., Shen, J., Han, W., Wang, L., 2018. Interfacial growth of metal–organic framework membranes on porous polymers via phase transformation. Chemical Communications 54 (29), 3590–3593.
Li, X., Liu, Y., Wang, J., Gascon, J., Li, J., Van der Bruggen, B., 2017b. Metal–organic frameworks based membranes for liquid separation. Chemical Society Reviews 46 (23), 7124–7144.
Li, X., Shi, T., Li, B., Chen, X., Zhang, C., Guo, Z., Zhang, Q., 2019b. Subtractive manufacturing of stable hierarchical micro-nano structures on AA5052 sheet with enhanced water repellence and durable corrosion resistance. Materials & Design 183, 108152.
Lim, I., Schrader, W., Schüth, F., 2015. Insights into the Molecular Assembly of Zeolitic Imidazolate Frameworks by ESI-MS. Chemistry of Materials 27, 3088–3095.
Lin, R., Hernandez, B.V., Ge, L., Zhu, Z., 2018. Metal organic framework based mixed matrix membranes: an overview on filler/polymer interfaces. Journal of Materials Chemistry A 6 (2), 293–312.
Lin, Y., Chen, Y., Wang, R., 2019b. Thin film nanocomposite hollow fiber membranes incorporated with surface functionalized HKUST-1 for highly-efficient reverses osmosis desalination process. Journal of Membrane Science 589, 117249. https://doi.org/10.1016/j.memsci.2019.117249.
Lin, Y., Wu, H.-C., Yasui, T., Yoshioka, T., Matsuyama, H., 2019a. Development of an HKUST-1 nanofiller-templated poly (ether sulfone) mixed matrix membrane for a highly efficient ultrafiltration process. ACS Applied Materials & Interfaces 11 (20), 18782–18796.
Ling, P., Lei, J., Zhang, L., Ju, H., 2015. Porphyrin-encapsulated metal-organic frameworks as mimetic catalysts for electrochemical DNA sensing via allosteric switch of hairpin DNA. Analytical Chemistry 87 (7), 3957–3963.
Liu, L., Luo, X.-B., Ding, L., Luo, S.-L., 2019. Application of nanotechnology in the removal of heavy metal from water. In: Nanomaterials for the removal of pollutants and resource reutilization. Elsevier, pp. 83–147.
Liu, Y., Ban, Y., Yang, W., 2017. Microstructural engineering and architectural design of metal–organic framework membranes. Advanced Materials 29 (31), 1606949.
Liu, X., Li, Y., Zhu, G., Ban, Y., Xu, L., Yang, W., 2011. An organophilic pervaporation membrane derived from metal–organic framework nanoparticles for efficient recovery of bio-alcohols. Angewandte Chemie 123 (45), 10824–10827.
Lovey, J., Shiny, J., Alen, V.L., 2020. Performance and antifouling behaviour of nanoclay incorporated polysulfone ultrafiltration membrane for wastewater treatment. Desalin. Water Treat 180, 37–42.
Lv, S.-W., Liu, J.-M., Ma, H., Wang, Z.-H., Li, C.-Y., Zhao, N., Wang, S., 2019. Simultaneous adsorption of methyl orange and methylene blue from aqueous solution using amino functionalized Zr-based MOFs. Microporous and Mesoporous Materials 282, 179–187.
Ma, D., Peh, S.B., Han, G., Chen, S.B., 2017a. Thin-film nanocomposite (TFN) membranes incorporated with super-hydrophilic metal–organic framework (MOF) UiO-66: toward enhancement of water flux and salt rejection. ACS Applied Materials & Interfaces 9 (8), 7523–7534.
Ma, J., Guo, X., Ying, Y., Liu, D., Zhong, C., 2017b. Composite ultrafiltration membrane tailored by MOF@GO with highly improved water purification performance. Chemical Engineering Journal 313, 890–898. https://doi.org/10.1016/j.cej.2016.10.127.
Ma, X., Chai, Y., Li, P., Wang, B., 2019. Metal–organic framework films and their potential applications in environmental pollution control. Accounts of Chemical Research 52 (5), 1461–1470.
Mahdavi, H., Karami, M., Heidari, A.A., kahriz, P.K., 2021. Preparation of mixed matrix membranes made up of polysulfone and MIL-53(Al) nanoparticles as promising membranes for separation of aqueous dye solutions. Separation and Purification Technology 274, 119033. https://doi.org/10.1016/j.seppur.2021.119033.
Makhetha, T.A., Moutloali, R.M., 2018. Antifouling properties of Cu(tpa)@GO/PES composite membranes and selective dye rejection. Journal of Membrane Science 554, 195–210. https://doi.org/10.1016/j.memsci.2018.03.003.
Mamah, S.C., Goh, P.S., Ismail, A.F., Suzaimi, N.D., Yogarathinam, L.T., Raji, Y.O., El-badawy, T.H., 2021. Recent development in modification of polysulfone membrane for water treatment application. Journal of Water Process Engineering 40, 101835. https://doi.org/10.1016/j.jwpe.2020.101835.
Mao, H., Zhen, H.-G., Ahmad, A., Zhang, A.-S., Zhao, Z.-P., 2019. In situ fabrication of MOF nanoparticles in PDMS membrane via interfacial synthesis for enhanced ethanol permselective pervaporation. Journal of Membrane Science 573, 344–358.
Márquez, A.G., Demessence, A., Platero-Prats, A.E., Heurtaux, D., Horcajada, P., Serre, C., Chang, J., Férey, G., Boissière, C., Grosso, D., 2012. Cover Picture: Green Microwave Synthesis of MIL-100 (Al, Cr, Fe) Nanoparticles for Thin-Film Elaboration (Eur. J. Inorg. Chem. 32/2012). European Journal of Inorganic Chemistry 32, 2012),n/a-n/a.
Marshall, C.R., Staudhammer, S.A., Brozek, C.K., 2019. Size control over metal–organic framework porous nanocrystals. Chem. Sci. 10 (41), 9396–9408. https://doi.org/10.1039/C9SC03802G.
McGuire, C.V., Forgan, R.S., 2015. The surface chemistry of metal–organic frameworks. Chemical Communications 51 (25), 5199–5217.
Mejia-Ariza, R., Huskens, J., 2016. The effect of PEG length on the size and guest uptake of PEG-capped MIL-88A particles. Journal of Materials Chemistry B 4 (6), 1108–1115.
Mohammad, A.W., Teow, Y.H., Ang, W.L., Chung, Y.T., Oatley-Radcliffe, D.L., Hilal, N., 2015. Nanofiltration membranes review: Recent advances and future prospects. Desalination 356, 226–254. https://doi.org/10.1016/j.desal.2014.10.043.
Mozafari, M., Seyedpour, S.F., Salestan, S.K., Rahimpour, A., Shamsabadi, A.A., Firouzjaei, M.D., Esfahani, M.R., Tiraferri, A., Mohsenian, H., Sangermano, M., 2019. Facile Cu-BTC surface modification of thin chitosan film coated polyethersulfone membranes with improved antifouling properties for sustainable removal of manganese. Journal of Membrane Science 117200.
Murray, C.B., Kagan, C.R., Bawendi, M.G., 2000. Synthesis and Characterization of Monodisperse Nanocrystals and Close-Packed Nanocrystal Assemblies. Annual Review of Materials Science 30 (1), 545–610. https://doi.org/10.1146/annurev.matsci.30.1.545.
Nakajima, N., Ikada, Y., 1995. Mechanism of amide formation by carbodiimide for bioconjugation in aqueous media. Bioconjugate Chemistry 6 (1), 123–130.
Nguyen, J.G., Cohen, S.M., 2010. Moisture-resistant and superhydrophobic metal-organic frameworks obtained via postsynthetic modification. Journal of the American Chemical Society 132 (13), 4560–4561.
Nune, S.K., Gunda, P., Thallapally, P.K., Lin, Y.-Y., Laird Forrest, M., Berkland, C.J., 2009. Nanoparticles for biomedical imaging. Expert Opinion on Drug Delivery 6 (11), 1175–1194.
Palit, S., 2016. Advanced environmental engineering separation processes, Environmental analysis and application of nanotechnology: A far-reaching review. In: Advanced Environmental Analysis. pp. 377–416.
Peng, Y., Li, Y., Ban, Y., Yang, W., 2017. Two-dimensional metal–organic framework nanosheets for membrane-based gas separation. Angewandte Chemie International

Edition 56 (33), 9757–9761.
Pouretedal, H.R., Sadegh, N., 2014. Effective removal of Amoxicillin, Cephalexin, Tetracycline and Penicillin G from aqueous solutions using activated carbon nanoparticles prepared from vine wood. Journal of Water Process Engineering 1, 64–73. https://doi.org/10.1016/j.jwpe.2014.03.006.
Pramono, E., Alfiansyah, R., Ahdiat, M., Wahyuningrum, D., Radiman, C.L., 2019. Hydrophilic poly(vinylidene fluoride)/bentonite hybrid membranes for microfiltration of dyes. Materials Research Express 6 (10), 105376. https://doi.org/10.1088/2053-1591/ab42e9.
Qian, X., Zhang, R., Chen, L., Lei, Y., Xu, A., 2019. Surface hydrophobic treatment of water-sensitive DUT-4 metal–organic framework to enhance water stability for hydrogen storage. ACS Sustainable Chemistry & Engineering 7 (19), 16007–16012.
Qiu, S., Xue, M., Zhu, G., 2014. Metal–organic framework membranes: from synthesis to separation application. Chemical Society Reviews 43 (16), 6116–6140.
Quist-Jensen, C.A., Macedonio, F., Drioli, E., 2015. Membrane technology for water production in agriculture: Desalination and wastewater reuse. Desalination 364, 17–32.
Rahimi, Z., Zinatizadeh, A.A., Zinadini, S., van Loosdrecht, M., Younesi, H., 2021. A new anti-fouling polysulphone nanofiltration membrane blended by amine-functionalized MCM-41 for post treating waste stabilization pond's effluent. Journal of Environmental Management 290, 112649. https://doi.org/10.1016/j.jenvman.2021.112649.
Rieter, W.J., Taylor, K.M.L., An, H., Lin, W., Lin, W., 2006. Nanoscale metal– organic frameworks as potential multimodal contrast enhancing agents. Journal of the American Chemical Society 128 (28), 9024–9025.
Ross, M.B., Ku, J.C., Lee, B., Mirkin, C.A., Schatz, G.C., 2016. Plasmonic metallurgy enabled by DNA. Advanced Materials 28 (14), 2790–2794.
Saeedi, M., Eslamifar, M., Khezri, K., Dizaj, S.M., 2019. Applications of nanotechnology in drug delivery to the central nervous system. Biomedicine & Pharmacotherapy 111, 666–675.
Saleem, H., Zaidi, S.J., 2020. Nanoparticles in reverse osmosis membranes for desalination: A state of the art review. Desalination 475, 114171. https://doi.org/10.1016/j.desal.2019.114171.
Samari, M., Zinadini, S., Zinatizadeh, A.A., Jafarzadeh, M., Gholami, F., 2020. Designing of a novel polyethersulfone (PES) ultrafiltration (UF) membrane with thermal stability and high fouling resistance using melamine-modified zirconium-based metal-organic framework (UiO-66-NH2/MOF). Separation and Purification Technology 251, 117010.
Sarici-Özdemir, Ç., Önal, Y., 2018. Study to observe the applicability of the adsorption isotherms used for the adsorption of medicine organics onto activated carbon. Particulate Science and Technology 36 (2), 254–261. https://doi.org/10.1080/02726351.2016.1246497.
Seoane, B., Dikhtiarenko, A., Mayoral, A., Tellez, C., Coronas, J., Kapteijn, F., Gascon, J., 2015. Metal organic framework synthesis in the presence of surfactants: towards hierarchical MOFs? CrystEngComm 17 (7), 1693–1700.
Seow, T.W., Lim, C.K., Nor, M.H.M., Mubarak, M.F.M., Lam, C.Y., Yahya, A., Ibrahim, Z., 2016. Review on wastewater treatment technologies. Int. J. Appl. Environ. Sci 11 (1), 111–126.
Sethupathy, M., Sethuraman, V., Manisankar, P., 2013. Preparation of PVDF/SiO 2 composite nanofiber membrane using electrospinning for polymer electrolyte analysis.
Seyedpour, S.F., Arabi Shamsabadi, A., Khoshhal Salestan, S., Dadashi Firouzjaei, M., Sharifian Gh, M., Rahimpour, A., Akbari Afkhami, F., Shirzad Kebria, M.reza, Elliott, M.A., Tiraferri, A., 2020a. Tailoring the Biocidal Activity of Novel Silver-Based Metal Azolate Frameworks. ACS Sustainable Chem. Eng.
Seyedpour, S.F., Dadashi Firouzjaei, M., Rahimpour, A., Zolghadr, E., Arabi Shamsabadi, A., Das, P., Akbari Afkhami, F., Sadrzadeh, M., Tiraferri, A., Elliott, M., 2020b. Toward Sustainable Tackling of Biofouling Implications and Improved Performance of TFC FO Membranes Modified by Ag-MOF Nanorods. ACS Applied Materials & Interfaces 12 (34), 38285–38298.
Seyedpour, S.F., Rahimpour, A., Najafpour, G., 2019. Facile in-situ assembly of silver-based MOFs to surface functionalization of TFC membrane: A novel approach toward long-lasting biofouling mitigation. Journal of Membrane Science 573, 257–269.
Seyedpour, S.F., Rahimpour, A., Shamsabadi, A.A., Soroush, M., 2018. Improved performance and antifouling properties of thin-film composite polyamide membranes modified with nano-sized bactericidal graphene quantum dots for forward osmosis. Chemical Engineering Research and Design 139, 321–334.
Seyedpour, S.F., Rahimpour, A., Esfahani, M.R., 2020c. Methods of making nanostructured metal-organic frameworks. Google Patents.
Shih, Y.-H., Lo, S.-H., Yang, N.-S., Singco, B., Cheng, Y.-J., Wu, C.-Y., Chang, I.-H., Huang, H.-Y., Lin, C.-H., 2012. Trypsin-Immobilized Metal–Organic Framework as a Biocatalyst In Proteomics Analysis. ChemPlusChem 77 (11), 982–986. https://doi.org/10.1002/cplu.201200186.
Shu, L., Xie, L.-H., Meng, Y., Liu, T., Zhao, C., Li, J.-R., 2020. A thin and high loading two-dimensional MOF nanosheet based mixed-matrix membrane for high permeance nanofiltration. Journal of Membrane Science 603, 118049.
Song, J.-L., Huang, Z.-Q., Mao, J., Chen, W.-J., Wang, B., Yang, F.-W., Liu, S.-H., Zhang, H.-J., Qiu, L.-P., Chen, J.-H., 2020. A facile synthesis of uniform hollow MIL-125 titanium-based nanoplatform for endosomal esacpe and intracellular drug delivery. Chemical Engineering Journal 396, 125246.
Sorribas, S., Gorgojo, P., Téllez, C., Coronas, J., Livingston, A.G., 2013. High flux thin film nanocomposite membranes based on metal–organic frameworks for organic solvent nanofiltration. Journal of the American Chemical Society 135 (40), 15201–15208.
Stassen, I., Burtch, N., Talin, A., Falcaro, P., Allendorf, M., Ameloot, R., 2017. An updated roadmap for the integration of metal–organic frameworks with electronic devices and chemical sensors. Chemical Society Reviews 46 (11), 3185–3241.
Stock, N., Biswas, S., 2011. Synthesis of metal-organic frameworks (MOFs): routes to various MOF topologies, morphologies, and composites. Chemical Reviews 112 (2), 933–969.
Stylianou, K.C., Imaz, I., Maspoch, D., 2011. Metal-Organic Frameworks: Nanoscale Frameworks. Encyclopedia of Inorganic and Bioinorganic Chemistry 1–19.
Sun, H., Tang, B., Wu, P., 2018. Hydrophilic hollow zeolitic imidazolate framework-8 modified ultrafiltration membranes with significantly enhanced water separation properties. Journal of Membrane Science 551, 283–293. https://doi.org/10.1016/j.memsci.2018.01.053.
Sun, M., Yan, L., Zhang, L., Song, L., Guo, J., Zhang, H., 2019. New insights into the rapid formation of initial membrane fouling after in-situ cleaning in a membrane bioreactor. Process Biochemistry 78, 108–113. https://doi.org/10.1016/j.procbio.2019.01.004.
Sun, Y., Sun, Q., Huang, H., Aguila, B., Niu, Z., Perman, J.A., Ma, S., 2017. A molecular-level superhydrophobic external surface to improve the stability of metal–organic frameworks. J. Mater. Chem. A 5 (35), 18770–18776. https://doi.org/10.1039/C7TA05800D.
Sun, Y., Zhang, R., Zhao, C., Wang, N., Xie, Y., Li, J.-R., 2014. Self-modified fabrication of inner skin ZIF-8 tubular membranes by a counter diffusion assisted secondary growth method. RSC Advances 4 (62), 33007–33012.
Surblé, S., Millange, F., Serre, C., Férey, G., Walton, R.I., 2006. An EXAFS study of the formation of a nanoporous metal–organic framework: evidence for the retention of secondary building units during synthesis. Chem. Commun. 14, 1518–1520. https://doi.org/10.1039/B600709K.
Talebian, S., Wallace, G.G., Schroeder, A., Stellacci, F., Conde, J., 2020. Nanotechnology-based disinfectants and sensors for SARS-CoV-2. Nature Nanotechnology 15 (8), 618–621.
Tang, J., Daiyan, R., Ghasemian, M.B., Idrus-Saidi, S.A., Zavabeti, A., Daeneke, T., Yang, J., Koshy, P., Cheong, S., Tilley, R.D., 2019. Advantages of eutectic alloys for creating catalysts in the realm of nanotechnology-enabled metallurgy. Nature Communications 10 (1), 1–14.
Taylor, K.M.L., Rieter, W.J., Lin, W., 2008. Manganese-based nanoscale metal– organic frameworks for magnetic resonance imaging. Journal of the American Chemical Society 130 (44), 14358–14359.
Thi Thanh Chau, V., Thi MinhThanh, H., Dinh Du, P., Thanh Tam Toan, T., Ngoc Tuyen, T., Xuan Mau, T., Quang Khieu, D., 2018. Metal-organic framework-101 (MIL-101): synthesis, kinetics, thermodynamics, and equilibrium isotherms of remazol deep black RGB adsorption. Journal of Chemistry, 2018.
Tilgner, D., Kempe, R., 2017. A Plasmonic Colloidal Photocatalyst Composed of a Metal–Organic Framework Core and a Gold/Anatase Shell for Visible-Light-Driven Wastewater Purification from Antibiotics and Hydrogen Evolution. Chemistry – A European Journal 23 (13), 3184–3190. https://doi.org/10.1002/chem.201605473.
Tsuruoka, T., Furukawa, S., Takashima, Y., Yoshida, K., Isoda, S., Kitagawa, S., 2009. Nanoporous nanorods fabricated by coordination modulation and oriented attachment growth. Angewandte Chemie 121 (26), 4833–4837.
Uemura, T., Hoshino, Y., Kitagawa, S., Yoshida, K., Isoda, S., 2006. Effect of organic polymer additive on crystallization of porous coordination polymer. Chemistry of Materials 18 (4), 992–995.
Uemura, T., Kitagawa, S., 2003. Prussian blue nanoparticles protected by poly (vinylpyrrolidone). Journal of the American Chemical Society 125 (26), 7814–7815.
Vatanpour, V., Esmaeili, M., Chahvari, S., Masteri-Farahani, M., 2021. Evaluation of morphology, performance and fouling tendency of mixed matrix PVDF ultrafiltration membranes incorporated by different size-controlled SAPO-34 nanozeolites. Journal of Environmental Chemical Engineering 9 (5), 105900. https://doi.org/10.1016/j.jece.2021.105900.
Vaucher, S., Li, M., Mann, S., 2000. Synthesis of Prussian blue nanoparticles and nanocrystal superlattices in reverse microemulsions. Angewandte Chemie International Edition 39 (10), 1793–1796.
Wang, C., Liu, C., Li, J., Sun, X., Shen, J., Han, W., Wang, L., 2017. Electrospun metal–organic framework derived hierarchical carbon nanofibers with high performance for supercapacitors. Chemical Communications 53 (10), 1751–1754.
Wang, C., Qian, X., An, X., 2015. In situ green preparation and antibacterial activity of copper-based metal–organic frameworks/cellulose fibers (HKUST-1/CF) composite. Cellulose 22 (6), 3789–3797.
Wang, K., Qin, Y., Quan, S., Zhang, Y., Wang, P., Liang, H., Ma, J., Cheng, X.Q., 2019. Development of highly permeable polyelectrolytes (PEs)/UiO-66 nanofiltration membranes for dye removal. Chemical Engineering Research and Design 147, 222–231. https://doi.org/10.1016/j.cherd.2019.05.014.
Wang, P., Li, Z., Xie, Q., Duan, W., Zhang, X., Han, H., 2021. A passive anti-icing strategy based on a superhydrophobic mesh with extremely low ice adhesion strength. Journal of Bionic Engineering 18 (1), 55–64.
Wang, M., Yang, L., Hu, B., Liu, J., He, L., Jia, Q., Song, Y., Zhang, Z., 2018a. Bimetallic NiFe oxide structures derived from hollow NiFe Prussian blue nanobox for label-free electrochemical biosensing adenosine triphosphate. Biosensors and Bioelectronics 113, 16–24. https://doi.org/10.1016/j.bios.2018.04.050.
Wang, S., McGuirk, C.M., d'Aquino, A., Mason, J.A., Mirkin, C.A., 2018b. Metal–organic framework nanoparticles. Advanced Materials 30 (37), 1800202.
cWang, X., Cheng, Q., Yu, Y., Zhang, X., 2018. Controlled nucleation and controlled growth for size predicable synthesis of nanoscale metal–organic frameworks (MOFs): a general and scalable approach. Angewandte Chemie International Edition 57 (26), 7836–7840.
Xu, Y., Peng, X., Tang, C.Y., Fu, Q.S., Nie, S., 2010. Effect of draw solution concentration and operating conditions on forward osmosis and pressure retarded osmosis performance in a spiral wound module. Journal of Membrane Science 348 (1), 298–309. https://doi.org/10.1016/j.memsci.2009.11.013.
Warsinger, D.M., Chakraborty, S., Tow, E.W., Plumlee, M.H., Bellona, C., Loutatidou, S.,

Karimi, L., Mikelonis, A.M., Achilli, A., Ghassemi, A., 2018. A review of polymeric membranes and processes for potable water reuse. Progress in Polymer Science 81, 209–237.
Webber, T.E., Liu, W.-G., Desai, S.P., Lu, C.C., Truhlar, D.G., Penn, R.L., 2017. Role of a Modulator in the Synthesis of Phase-Pure NU-1000. ACS Applied Materials & Interfaces 9 (45), 39342–39346.
Wen, Y., Chen, Y., Wu, Z., Liu, M., Wang, Z., 2019. Thin-film nanocomposite membranes incorporated with water stable metal-organic framework CuBTTri for mitigating biofouling. Journal of Membrane Science 582, 289–297.
Wibowo, A., Marsudi, M.A., Pramono, E., Belva, J., Parmita, A.W.Y.P., Patah, A., Eddy, D.R., Aimon, A.H., Ramelan, A., 2021. Recent Improvement Strategies on Metal-Organic Frameworks as Adsorbent, Catalyst, and Membrane for Wastewater Treatment. Molecules 26 (17), 5261. https://www.mdpi.com/1420-3049/26/17/5261.
Wilson, M., Barrientos-Palomo, S.N., Stevens, P.C., Mitchell, N.L., Oswald, G., Nagaraja, C.M., Badyal, J.P.S., 2018. Substrate-independent epitaxial growth of the metal–organic framework MOF-508a. ACS Applied Materials & Interfaces 10 (4), 4057–4065.
Xiao, F., Hu, X., Chen, Y., Zhang, Y., 2019. Porous Zr-based metal-organic frameworks (Zr-MOFs)-Incorporated thin-film nanocomposite membrane toward enhanced desalination performance. ACS Applied Materials & Interfaces 11 (50), 47390–47403.
Xie, J., Zhang, X., Wang, H., Zheng, H., Huang, Y., 2012. Analytical and environmental applications of nanoparticles as enzyme mimetics. TrAC Trends in Analytical Chemistry 39, 114–129.
Yan, X., Huang, X., Chen, Y., Liu, Y., Xia, L., Zhang, T., Lin, H., Jia, D., Zhong, B., Wen, G., Zhou, Y., 2021. A theoretical strategy of pure carbon materials for lightweight and excellent absorption performance. Carbon 174, 662–672. https://doi.org/10.1016/j.carbon.2020.11.044.
Yang, F., Efome, J.E., Rana, D., Matsuura, T., Lan, C., 2018. Metal–organic frameworks supported on nanofiber for desalination by direct contact membrane distillation. ACS Applied Materials & Interfaces 10 (13), 11251–11260.
Yang, L., Wang, Z., Zhang, J., 2017. Zeolite imidazolate framework hybrid nanofiltration (NF) membranes with enhanced permselectivity for dye removal. Journal of Membrane Science 532, 76–86. https://doi.org/10.1016/j.memsci.2017.03.014.
Yang, L., Zhao, T., Boldog, I., Janiak, C., Yang, X.-Y., Li, Q., Zhou, Y.-J., Xia, Y., Lai, D.-W., Liu, Y.-J., 2019a. Benzoic acid as a selector–modulator in the synthesis of MIL-88B (Cr) and nano-MIL-101(Cr). Dalton Trans 48 (3), 989–996. https://doi.org/10.1039/C8DT04186E.
Yang, S., Zou, Q., Wang, T., Zhang, L., 2019b. Effects of GO and MOF@GO on the permeation and antifouling properties of cellulose acetate ultrafiltration membrane. Journal of Membrane Science 569, 48–59. https://doi.org/10.1016/j.memsci.2018.09.068.
Yao, Y., et al., 2021. Macroscopic MOF architectures: effective strategies for practical application in water treatment. Small. n/a 2104387. https://doi.org/10.1002/smll.202104387.
Yi, B., Wong, Y.-L., Hou, C., Zhang, J., Xu, Z., Yao, X., 2021. Coordination-Driven Assembly of Metal–Organic Framework Coating for Catalytically Active Superhydrophobic Surface. Advanced Materials Interfaces 8 (2). https://doi.org/10.1002/admi.202001202.
Yi, F., Chen, D., Wu, M., Han, L., Jiang, H., 2016. Chemical sensors based on metal–organic frameworks. ChemPlusChem 81 (8), 675–690.
Ying, Y., Liu, D., Zhang, W., Ma, J., Huang, H., Yang, Q., Zhong, C., 2017. High-flux graphene oxide membranes intercalated by metal–organic framework with highly selective separation of aqueous organic solution. ACS Applied Materials & Interfaces 9 (2), 1710–1718.
Zango, Z.U., Jumbri, K., Sambudi, N.S., Ramli, A., Abu Bakar, N.H.H., Saad, B., Rozaini, M.N.H., Isiyaka, H.A., Jagaba, A.H., Aldaghri, O., Sulieman, A., 2020. A Critical Review on Metal-Organic Frameworks and Their Composites as Advanced Materials for Adsorption and Photocatalytic Degradation of Emerging Organic Pollutants from Wastewater. Polymers 12 (11). https://doi.org/10.3390/polym12112648.
Zahid, M., Rashid, A., Akram, S., Rehan, Z.A., Razzaq, W., 2018. A comprehensive review on polymeric nano-composite membranes for water treatment. J. Membr. Sci. Technol 8 (1), 1–20.
Zhang, H., Guan, W., Zhang, L., Guan, X., Wang, S., 2020. Degradation of an Organic Dye by Bisulfite Catalytically Activated with Iron Manganese Oxides: The Role of Superoxide Radicals. ACS Omega 5 (29), 18007–18012.
Zhang, H., Sun, M., Song, L., Guo, J., Zhang, L., 2019c. Fate of NaClO and membrane foulants during in-situ cleaning of membrane bioreactors: Combined effect on thermodynamic properties of sludge. Biochemical Engineering Journal 147, 146–152. https://doi.org/10.1016/j.bej.2019.04.016.
Zhang, K., Huo, Q., Zhou, Y.-Y., Wang, H.-H., Li, G.-P., Wang, Y.-W., Wang, Y.-Y., 2019b. Textiles/metal–organic frameworks composites as flexible air filters for efficient particulate matter removal. ACS Applied Materials & Interfaces 11 (19), 17368–17374.
Zhang, L., He, Y., Luo, P., Ma, L., Li, S., Nie, Y., Zhong, F., Wang, Y., Chen, L., 2022. Photocatalytic GO/M88A "interceptor plate" assembled nanofibrous membrane with photo-Fenton self-cleaning performance for oil/water emulsion separation. Chemical Engineering Journal 427, 130948. https://doi.org/10.1016/j.cej.2021.130948.
Zhang, X., Li, Y., Van Goethem, C., Wan, K., Zhang, W., Luo, J., Vankelecom, I.F.J., Fransaer, J., 2019a. Electrochemically assisted interfacial growth of MOF membranes. Matter 1 (5), 1285–1292.
Zhang, Y.-Z., He, T., Kong, X.-J., Lv, X.-L., Wu, X.-Q., Li, J.-R., 2018. Tuning water sorption in highly stable Zr (IV)-metal–organic frameworks through local functionalization of metal clusters. ACS Applied Materials & Interfaces 10 (33), 27868–27874.
Zhao, P., Li, R., Wu, W., Wang, J., Liu, J., Zhang, Y., 2019b. In-situ growth of polyvinylpyrrolidone modified Zr-MOFs thin-film nanocomposite (TFN) for efficient dyes removal. Composites Part B: Engineering 176, 107208. https://doi.org/10.1016/j.compositesb.2019.107208.
Zhao, T., Li, S.-H., Shen, L., Wang, Y., Yang, X.-Y., 2018b. The sized controlled synthesis of MIL-101(Cr) with enhanced CO2 adsorption property. Inorganic Chemistry Communications 96, 47–51. https://doi.org/10.1016/j.inoche.2018.07.036.
Zhao, T., Yang, L., Feng, P., Gruber, I., Janiak, C., Liu, Y., 2018a. Facile synthesis of nano-sized MIL-101(Cr) with the addition of acetic acid. Inorganica Chimica Acta 471, 440–445. https://doi.org/10.1016/j.ica.2017.11.030.
Zhao, Y., Liu, Y., Wang, X., Huang, X., Xie, Y.F., 2019a. Impacts of metal–organic frameworks on structure and performance of polyamide thin-film nanocomposite membranes. ACS Applied Materials & Interfaces 11 (14), 13724–13734.
Zheng, G., Yao, L., You, X., Liao, Y., Wang, R., Huang, J.J., 2021a. Effects of different secondary nano-scaled roughness on the properties of omniphobic membranes for brine treatment using membrane distillation. Journal of Membrane Science 620, 118918. https://doi.org/10.1016/j.memsci.2020.118918.
Zheng, H., Wang, D., Sun, X., Jiang, S., Liu, Y., Zhang, D., Zhang, L., 2021b. Surface modified by green synthetic of Cu-MOF-74 to improve the anti-biofouling properties of PVDF membranes. Chemical Engineering Journal 411, 128524. https://doi.org/10.1016/j.cej.2021.128524.
Zheng, Y., Qiao, S.-Z., 2017. Direct growth of well-aligned MOF arrays onto various substrates. Chem 2 (6), 751–752.
Zhou, S., Gao, J., Zhu, J., Peng, D., Zhang, Y., Zhang, Y., 2020. Self-cleaning, antibacterial mixed matrix membranes enabled by photocatalyst Ti-MOFs for efficient dye removal. Journal of Membrane Science 610, 118219.
Zhou, Z., Wu, X.-F., 2015. Electrospinning superhydrophobic–superoleophilic fibrous PVDF membranes for high-efficiency water–oil separation. Materials Letters 160, 423–427.
Zhuang, J., Kuo, C.-H., Chou, L.-Y., Liu, D.-Y., Weerapana, E., Tsung, C.-K., 2014. Optimized metal–organic-framework nanospheres for drug delivery: evaluation of small-molecule encapsulation. ACS Nano 8 (3), 2812–2819.
Zimpel, A., Röder, T.P.R., Engelke, H., Ingrisch, M., Peller, M., Rädler, J.O., Wagner, E., Bein, T., Lächelt, U., Wuttke, S., 2016. Imparting Functionality to MOF Nanoparticles by External Surface Selective Covalent Attachment of Polymers. Chemistry of Materials 28, 3318–3326.
Zirehpour, A., Rahimpour, A., Ulbricht, M., 2017. Nano-sized metal organic framework to improve the structural properties and desalination performance of thin film composite forward osmosis membrane. Journal of Membrane Science 531, 59–67.
Zornoza, B., Tellez, C., Coronas, J., Gascon, J., Kapteijn, F., 2013. Metal organic framework based mixed matrix membranes: An increasingly important field of research with a large application potential. Microporous and Mesoporous Materials 166, 67–78.